MOLECULAR AND CELLULAR BIOLOGY, Apr. 1996, p. 1376–1390 Vol. 16, No. 4
0270-7306/96/$04.00+0

The LIM Domain-Containing Dbm1 GTPase-Activating Protein Is Required for Normal Cellular Morphogenesis in *Saccharomyces cerevisiae*

GUANG-CHAO CHEN, LI ZHENG, AND CLARENCE S. M. CHAN*

Department of Microbiology, The University of Texas, Austin, Texas 78712

Received 19 September 1995/Returned for modification 2 November 1995/Accepted 16 January 1996

Normal cell growth in the yeast *Saccharomyces cerevisiae* involves the selection of genetically determined bud sites where most growth is localized. Previous studies have shown that *BEM2*, which encodes a GTPase-activating protein (GAP) that is specific for the Rho-type GTPase Rho1p in vitro, is required for proper bud site selection and bud emergence. We show here that *DBM1*, which encodes another putative Rho-type GAP with two tandemly arranged cysteine-rich LIM domains, also is needed for proper bud site selection, as haploid cells lacking Dbm1p bud predominantly in a bipolar, rather than the normal axial, manner. Furthermore, yeast cells lacking both Bem2p and Dbm1p are inviable. The nonaxial budding defect of *dbm1* mutants can be rescued partially by overproduction of Bem3p and is exacerbated by its absence. Since Bem3p has previously been shown to function as a GAP for Cdc42p, and also less efficiently for Rho1p, our results suggest that Dbm1p, like Bem2p and Bem3p, may function in vivo as a GAP for Cdc42p and/or Rho1p. Both LIM domains of Dbm1p are essential for its normal function. Point mutations that alter single conserved cysteine residues within either LIM domain result in mutant forms of Dbm1p that can no longer function in bud site selection but instead are capable of rescuing the inviability of *bem2* mutants at 35°C.

Cell growth in the budding yeast *Saccharomyces cerevisiae* is a highly polarized process (reviewed in references 12 and 41). Initiation of growth involves the selection of a proper bud site on the surface of the ellipsoidal mother cell. The choice of this bud site is nonrandom (10, 14, 16, 23, 25, 42, 61). Under commonly used laboratory culture conditions, most wild-type haploid cells bud from only one pole in an axial fashion (i.e., from sites near the site of the previous cell division), whereas wild-type **a**/α diploid cells bud in a bipolar fashion, with mother cells budding from either pole and daughter cells budding preferentially from the pole opposite the site of the previous cell division. After the selection of a bud site, subsequent growth is localized mostly to this selected site, eventually giving rise to a bud that becomes the daughter cell after cytokinesis.

At least two classes of genes have been identified as being important for proper bud site selection in haploid cells. The first class includes *BUD3*, *BUD4* (14), *LYT1* (47), *CDC3*, *CDC10*, *CDC11*, *CDC12* (15, 21), and *AXL1* (24). Haploid cells carrying mutations in these genes often bud in a bipolar instead of the normal axial fashion. Cdc3p, Cdc10p, Cdc11p, and Cdc12p are putative components of the 10-nm neck filaments that are required for cytokinesis, and they are found at presumptive bud sites early in the cell cycle (22, 26, 32). Bud3p is similarly localized during part of the cell cycle (15). These proteins may mark the site for axial budding. Axl1p is a putative protease (24); however, the protease activity of Axl1p appears not to be essential for its function in bud site selection (1). The second class of genes includes *RSR1*/*BUD1*, *BUD2*, *BUD5* (7, 13, 14), and *SPA2* (72). The pattern of bud site selection in haploid cells carrying mutations in these genes becomes randomized, often being neither axial nor bipolar. Rsr1p/Bud1p is a Ras-related GTPase that is regulated by the Bud2 GTPase-activating protein (GAP), the Bud5 GDP-GTP exchange factor (5, 8, 13, 54, 56), and possibly Cdc24p (see below), which can function in vitro as a GTPase-inhibiting protein for Rsr1p/Bud1p (82). Spa2p is a protein that is concentrated at regions of active cell surface growth (72, 73). Mutations in both classes of genes mentioned above do not prevent the localization of growth to the inappropriately selected bud sites.

Once a bud site has been selected, several other genes are known to be required for the subsequent localization of growth to this site (bud emergence). They include *BEM1*, *BEM2* (6, 11, 13, 33, 55), *CDC24* (51, 70, 71), *CDC42*, and *CDC43* (2, 52). Mutations in these genes result in large, multinucleate, unbudded cells that in most cases have also been shown to exhibit delocalized cell surface growth. Cdc42p is a Rho-type GTPase (30) that is regulated by the Cdc24 GDP-GTP exchange factor (7, 83, 85), the Cdc43-Ram2 geranylgeranyltransferase I (53, 76), and possibly the Bem3 protein (83, 84). The latter protein functions in vitro as a GAP for Cdc42p, and less efficiently for Rho1p, another Rho-type GTPase that is needed for bud growth but not bud emergence (40, 81). Bem1p is an SH3 domain-containing protein (17) that can bind to Cdc24p (55) and is found at regions of active cell surface growth (17a); the properties of Bem2p will be described below.

The Rho-type GTPases and their regulatory proteins mentioned above, like their mammalian counterparts, may function at least in part to regulate the yeast actin cytoskeleton (reviewed in references 27 and 75), which is organized in a highly polarized fashion (9, 78). A functional actin cytoskeleton is important for polarized cell growth, probably because it serves to target secretory vesicles to growth sites. Mutants defective in some Rho-type GTPases and their regulatory proteins (e.g., Bem2p, Cdc24p, Cdc42p, Rho3p, and Rho4p) are defective in the organization of the yeast actin cytoskeleton (2, 3, 33, 44, 77, 86). Furthermore, the Rho1 and Cdc42 GTPases, like cortical actin patches, are concentrated at regions of active cell surface growth (81, 87), and the ability of permeabilized *cdc42-1* mutant cells to assemble cortical actin patches in vitro is greatly reduced (39).

* Corresponding author. Phone: (512)-471-6860. Fax: (512)-471-7088. Electronic mail address: clarence_chan@mail.utexas.edu.

TABLE 1. Yeast Strains used in this study[a]

Strain	Genotype
DBY1830	**a**/α *ade2*/+ *lys2-801*/+ *his3-Δ200*/*his3-Δ200 ura3-52*/*ura3-52 leu2-3,112*/*leu2-3,112 trp1-1*/*trp1-1*
CBY1830-30	**a**/α *ade2*/+ *lys2-801*/+ *his3-Δ200*/*his3-Δ200 ura3-52*/*ura3-52 leu2-3,112*/*leu2-3,112 trp1-1*/*trp1-1 bem2-Δ103*::*LEU2*/+
CBY1830-30-13	**a**/α *ade2*/+ *lys2-801*/+ *his3-Δ200*/*his3-Δ200 ura3-52*/*ura3-52 leu2-3,112*/*leu2-3,112 trp1-1*/*trp1-1 bem2-Δ103*::*LEU2*/+ *dbm1-3*::*HIS3*/+
CBY1830-44	**a**/α *ade2*/+ *lys2-801*/+ *his3-Δ200*/*his3-Δ200 ura3-52*/*ura3-52 leu2-3,112*/*leu2-3,112 trp1-1*/*trp1-1 dbm1-3*::*HIS3*/+
CBY1830-45	**a**/α *ade2*/+ *lys2-801*/+ *his3-Δ200*/*his3-Δ200 ura3-52*/*ura3-52 leu2-3,112*/*leu2-3,112 trp1-1*/*trp1-1 dbm1-Δ4*::*HIS3*/+
CBY1830-45-1	**a**/α *ade2*/+ *lys2-801*/+ *his3-Δ200*/*his3-Δ200 ura3-52*/*ura3-52 leu2-3,112*/*leu2-3,112 trp1-1*/*trp1-1 dbm1-Δ4*::*HIS3*/+ *bem3*::*LEU2*/+
CBY1830-47	**a**/α *ade2*/+ *lys2-801*/+ *his3-Δ200*/*his3-Δ200 ura3-52*/*ura3-52 leu2-3,112*/*leu2-3,112 trp1-1*/*trp1-1 dbm1-Δ4*::*HIS3*/+
CCY109-9C-1	α *ade2 his3-Δ200 ura3-52 lys2-Δ101*::*HIS3*::*lys2-Δ102 bem2-101*
CCY109-9C-1*	α *ade2 his3-Δ200 ura3-52 lys2-Δ101*::*HIS3*::*lys2-Δ102 bem2-101 DBM1-1*
CCY109-9C-1**	α *ade2 his3-Δ200 ura3-52 lys2-Δ101*::*HIS3*::*lys2-Δ102 bem2-101 DBM1-2*
CCY334-6C	α *his3-Δ200 ura3-52 lys2-801 leu2-3,112 trp1-1 bem2-Δ103*::*LEU2* with pCC231 (*BEM2 URA3*)
CCY416-12D	α *his3-Δ200 ura3-52 lys2-801 leu2-3,112 trp1-1 bem2-101*
CCY432-15C	**a** *his3-Δ200 ura3-52 lys2-801 leu2-3,112 bem2-101 URA3* (at *SPT2*)
CCY447-5C	**a** *ade2 his3-Δ200 ura3-52 lys2-Δ101*::*HIS3*::*lys2-Δ102 leu2-3,112 bem2-101 DBM1-1*
CCY447-10C	α *ade2 his3-Δ200 ura3-52 lys2-Δ101*::*HIS3*::*lys2-Δ102 leu2-3,112 bem2-101 DBM1-1*
CCY482-13D	**a** *ade2 his3-Δ200 ura3-52 lys2-Δ101*::*HIS3*::*lys2-Δ102 leu2-3,112*
CCY578-6A	α *ade2 his3-Δ200 ura3-52 bem2-101*
CCY666-7B	α *ade2 his3-Δ200 ura3-52 leu2-3,112*
CCY695-10C	**a** *ade2 his3-Δ200 ura3-52 lys2-Δ101*::*HIS3*::*lys2-Δ102 leu2-3,112 bem2-101 DBM1-2*
CCY814-3A	**a** *ade2 his3-Δ200 ura3-52 leu2-3,112 trp1-1 dbm1-3*::*HIS3*
CCY825	**a**/α *ade2*/+ *his3-Δ200*/*his3-Δ200 ura3-52*/*ura3-52 leu2-3,112*/*leu2-3,112 bem2-Δ103*::*LEU2*/+
CCY825-2	**a**/α *ade2*/+ *his3-Δ200*/*his3-Δ200 ura3-52*/*ura3-52 leu2-3,112*/*leu2-3,112 bem2-Δ103*::*LEU2*/+ *dbm1-Δ4*::*HIS3*/+
CCY862-5B	**a** *ade2 his3-Δ200 ura3-52 leu2-3,112 dbm1-Δ4*::*HIS3*
CCY864-5A	α *ade2 his3-Δ200 ura3-52 leu2-3,112 DBM1-1*
CCY864-5D	**a** *ade2 his3-Δ200 ura3-52 lys2-Δ101*::*HIS3*::*lys2-Δ102 leu2-3,112 DBM1-1*
CCY886-4C	**a** *ade2 his3-Δ200 ura3-52 lys2-Δ101*::*HIS3*::*lys2-Δ102 leu2-3,112 bem2-Δ103*::*LEU2 DBM1-1*
CCY890-12C	**a** *ade2 his3-Δ200 ura3-52 leu2-3,112 trp1-1 dbm1-Δ4*::*HIS3*
CCY898-25A	α *his3-Δ200 ura3-52 lys2-801 leu2-3,112 trp1-1 bem3*::*LEU2*
CCY898-25B	α *his3-Δ200 ura3-52 lys2-801 leu2-3,112 trp1-1*
CCY898-25C	**a** *ade2 his3-Δ200 ura3-52 leu2-3,112 trp1-1 dbm1-Δ4*::*HIS3*
CCY898-25D	**a** *ade2 his3-Δ200 ura3-52 leu2-3,112 trp1-1 dbm1-Δ4*::*HIS3 bem3*::*LEU2*
CCY907-16A	**a** *ade2 his3-Δ200 ura3-52 lys2-Δ101*::*HIS3*::*lys2-Δ102 leu2-3,112 bem2-Δ103*::*LEU2 DBM1-2*
CCY910-9D	α *ade2 his3-Δ200 ura3-52 lys2-801 bem2-101*
CCY910-12C	**a** *ade2 his3-Δ200 ura3-52 lys2-Δ101*::*HIS3*::*lys2-Δ102 leu2-3,112 bem2-101*
CCY919-11B	**a** *ade2 his3-Δ200 ura3-52 lys2-Δ101*::*HIS3*::*lys2-Δ102 leu2-3,112 DBM1-2*
CCY926-2D	**a** *ade2 his3-Δ200 ura3-52 lys2-Δ101*::*HIS3*::*lys2-Δ102 leu2-3,112 bem2-Δ103*::*LEU2*

[a] Most of the strains were constructed specifically for this study, the exception being DBY1830, which is from D. Botstein's laboratory collection. The origins of some of the markers used are indicated in the text. CBY1830-45 and CBY1830-47 differ in that the *dbm1-Δ4*::*HIS3* mutation is tightly linked to the *ade2* locus in CBY1830-45, whereas the *dbm1-Δ4*::*HIS3* mutation is tightly linked to the *ADE2* locus in CBY1830-47.

Among the many yeast proteins known to be involved in cellular morphogenesis, Bem2p (and Cdc24p) is unique in that in addition to its role in bud emergence described above, it is also required for proper bud site selection. At permissive growth temperatures, temperature-sensitive *bem2* mutants have randomized budding patterns, whereas at restrictive growth temperatures, these mutants are defective in bud emergence, organization of the actin cytoskeleton, and localized cell surface growth, thus becoming arrested as large, round, multinucleate cells that are mostly unbudded (6, 11, 33, 55, 77). This unique property suggests that Bem2p may serve to link protein components involved in bud site selection to those involved in bud emergence. The COOH-terminal 201 residues of Bem2p function in vitro as a GAP for the Rho1 but not the Cdc42 Rho-type GTPase (55, 83, 84), and the temperature-sensitive (Ts^-) growth phenotype as well as the randomized bud site selection defect of *bem2* mutants can be suppressed partially (rather than enhanced) by an increase in the dosage of the gene encoding the Rho1 or Rho2, but not the Rho3, Rho4, or Cdc42, GTPase (33). Furthermore, certain combinations of *bem2* and *rho1* mutations result in a synthetic lethal phenotype (77). These results together suggest that Bem2p potentially may function in vivo as a GAP for Rho1p and Rho2p and that controlled cycling between the GTP- and GDP-bound states may be important for Rho1p and Rho2p function (33). To identify other genes that may function with *BEM2* in the control of cellular morphogenesis, we have identified suppressor mutations of *bem2*. Results from the analysis of one such gene, *DBM1*, will be described in this report.

MATERIALS AND METHODS

Strains, media, and genetic techniques. The yeast strains used in this study are listed in Table 1. The diploid strains CBY1830-44 and CBY1830-30-13 were constructed by a one-step gene disruption procedure (64), replacing one of the two *DBM1* genes in DBY1830 and CBY1830-30, respectively, with the *dbm1-3*::*HIS3* allele present on pCC592. The diploid strains CBY1830-45, CBY1830-47, and CCY825-2 were similarly constructed, replacing one of the two *DBM1* genes in DBY1830 (for CBY1830-45 and CBY1830-47) or CCY825 (for CCY825-2) with the *dbm1-Δ4*::*HIS3* allele present on pCC735. The diploid strain CBY1830-45-1 was constructed by replacing one of the two *BEM3* genes in CBY1830-45 with the *bem3*::*LEU2* allele present on pPB432 (gift of A. Bender). These gene disruptions were confirmed by DNA hybridization. Haploid *dbm1-3*::*HIS3* and *dbm1-Δ4*::*HIS3* strains were generated from CBY1830-44, CBY1830-45, and CBY1830-47. *Escherichia coli* DB1142 (*leu pro thr hsdR hsdM recA*) was used routinely as a host for plasmids, except in experiments for site-directed mutagenesis, in which case strain CJ236 (*dut-1 ung-1 thi-1 relA1* with pCJ105 [Cm^r]) was used as a host for the preparation of deoxyuracil-containing plasmid DNA and BSJ72 {*supE hsdΔ5 thi*(Δ*lac-proAB*) λ^r Sm^r F′ [*traD36 proAB*$^+$ *lacI*^{q} *lacZΔM15*]} was used as a host for the preparation of mutagenized plasmids.

Rich medium (YEPD), synthetic minimal medium (SD), and SD with necessary supplements were prepared as described elsewhere (63). Cells were routinely grown at 26°C unless otherwise specified. Yeast genetic manipulations were performed as described by Rose et al. (63).

Isolation of *DBM1-1* and *DBM1-2* mutants. Spontaneous temperature-resistant (Ts^+) revertants of haploid *bem2-101* Ts^- mutants (CCY109-9C-1) were identified as described previously (33). Extragenic suppressors were identified by tetrad analysis after mating revertants to a *bem2-101* strain (CCY432-15C) that carried a *URA3* marker next to the *SPT2* locus, which is tightly linked to *bem2-101* (11). Diploids obtained from these matings were also used to test dominance of the suppression phenotype. This analysis yielded the dominant *DBM1-1* and *DBM1-2* suppressor mutations.

Molecular cloning of the *DBM1* and *DBM1-1* alleles. The dominant *DBM1-1* mutant allele was cloned on the basis of its ability to suppress the Ts^- phenotype of *bem2-101* mutants even in the presence of the wild-type *DBM1* gene. Genomic DNA from a *bem2-101 DBM1-1* strain (CCY447-10C) was isolated (43) and partially digested with the restriction enzyme *Sau*3A. DNA fragments of ~10 kb were purified from an agarose gel and ligated into the *Bam*HI site of the low-copy-number *URA3*-CEN plasmid pRS316 (69). The ligated DNA was transformed into *E. coli* DB1142 to generate a yeast genomic library. DNA from this library was used to transform a *ura3 bem2-101 DBM1* strain (CCY578-6A). Ura^+ transformants were selected by plating cells on supplemented SD lacking uracil. After 17 h at 26°C, plates containing Ura^+ transformants were shifted to 37°C. After 3 more days, Ts^+ Ura^+ transformants were identified, and plasmids were recovered from such transformants into *E. coli* DB1142. The ability of these recovered plasmids to suppress the Ts^- phenotype of *bem2-101 DBM1* mutants (CCY578-6A) was retested.

The wild-type *DBM1* gene was cloned on the basis of its physical proximity to the *ADE2* gene. Plasmids containing *ADE2* (and flanking sequences) were isolated by transforming the *ade2 ura3* (*bem2-101*) strain CCY578-6A with a yeast wild-type genomic library constructed in the low-copy-number *URA3*-CEN plasmid YCp50 (62). Ade^+ Ura^+ transformants were selected by plating cells on supplemented SD lacking adenine and uracil at 26°C. Plasmids were recovered from Ade^+ Ura^+ transformants into *E. coli* DB1142 and analyzed.

DNA manipulation. Functional localization of the cloned *DBM1-1* suppressor gene was done by subcloning DNA fragments into the low-copy-number *URA3*-CEN plasmid pRS316 (69) or YCp50 (62). pCC592, carrying the *dbm1-3*::*HIS3* mutant allele, was constructed by inserting the ~1.7-kb *Bam*HI fragment (containing *HIS3*) of pJJ215 (31) into the unique *Bgl*II site of the low-copy-number *URA3*-CEN plasmid pCC581. pCC735, carrying the *dbm1*-Δ*4*::*HIS3* mutant allele, was constructed by replacing the DNA sequence between the *Xho*I and *Bgl*II sites present in the low-copy-number *URA3*-CEN plasmid pCC734 with the ~1.3-kb *Xho*I-*Bam*HI fragment (containing *HIS3*) of pJJ215 (31). Molecular analysis of the cloned wild-type *DBM1* gene was done by subcloning DNA fragments into the low-copy-number *URA3*-CEN plasmid pRS316 or the high-copy-number *URA3*-2μm plasmid pSM217 (69). The plasmid pCC709 was created by ligating the ~1.5-kb *Xba*I DNA fragment (carrying the 3′ 44% of the wild-type *DBM1* coding sequence) of pCC691 into the *Xba*I site of pRS316.

dbm1 mutant alleles carrying mutation(s) in the LIM domains were created by site-directed mutagenesis (36) of wild-type *DBM1* present on the high-copy-number *URA3*-2μm plasmid pCC707 with the degenerate primers SIP24.7p (5′-GCTTAATGGTTTCTCAC[A/T]TTTGTAAC[A/T]AGCGAAACA-3′) and/or SIP24.8p (5′-GCAATATTTTCACCAC[A/T]TTTACAGC[A/T]TTTAAAACA-3′) (mutagenic bases are underlined). The *Xho*I-*Hin*dIII fragments carrying these mutant alleles were subsequently recloned into the low-copy-number *URA3*-CEN plasmid pRS316 (69) to generate plasmids pCC795 to pCC801.

Antibody production. Plasmid pCC741 was constructed by inserting the 2.2-kb *Bam*HI-*Hin*dIII DNA fragment of pCC707, containing the COOH-terminal 64% of the *DBM1* coding sequence, into the *Bam*HI-*Hin*dIII sites of the TrpE fusion protein vector pATH10 (34), thus creating an in-frame fusion between *trpE* and *DBM1*. The TrpE-Dbm1 fusion protein was partially purified as an insoluble protein from *E. coli* cells harboring pCC741 (34) and was further purified on preparative sodium dodecyl sulfate (SDS)-polyacrylamide gels. The partially pure TrpE-Dbm1 fusion protein was then transferred to nitrocellulose membrane and solubilized in dimethyl sulfoxide (Sigma Chemical Co., St. Louis, Mo.) for use as an antigen in rabbits. Antibodies were affinity purified as described previously (57, 79) except that nitrocellulose membrane fragments were also used for the immunodepletion of the crude sera and the TrpE-Dbm1 fusion protein used for the adsorption of anti-Dbm1 antibodies was immobilized on a polyvinylidene difluoride membrane (Millipore Co., Bedford, Mass.). For immunoblotting experiments, yeast cell lysates were also transferred onto a polyvinylidene difluoride membrane.

Cytological techniques. Immunofluorescence staining of yeast cells was carried out as described previously (57). Actin was stained with affinity-purified guinea pig anti-actin antibodies (48) and affinity-purified fluorescein isothiocyanate-conjugated goat anti-guinea pig secondary antibodies (Organon Teknika Corp., West Chester, Pa.). DNA was stained with 4′,6-diamidino-2-phenylindole (DAPI; 1 μg/ml; Accurate Chemical Co., Westbury, N.Y.), and chitin was stained with Calcofluor (0.2 mg/ml; Sigma). Stained cells were viewed with a Zeiss Axioskop fluorescence microscope and photographed with Kodak TMAX 400 film.

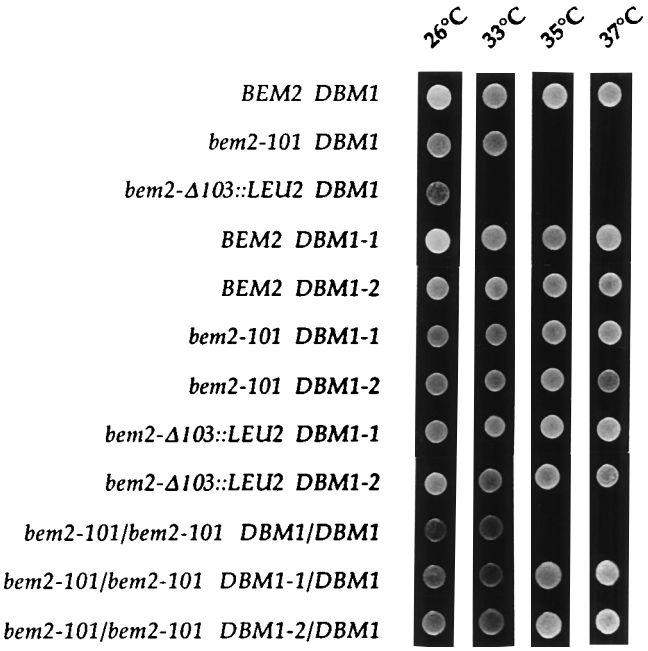

FIG. 1. Suppression of the Ts^- growth phenotype of *bem2* mutants by the *DBM1-1* and *DBM1-2* mutations. Suspensions of yeast cells were spotted on YEPD plates and allowed to grow at the indicated temperatures for 1.75 days. The yeast strains used were CCY482-13D (*BEM2 DBM1*), CCY910-12C (*bem2-101 DBM1*), CCY926-2D (*bem2-Δ103::LEU2 DBM1*), CCY864-5D (*BEM2 DBM1-1*), CCY919-11B (*BEM2 DBM1-2*), CCY447-5C (*bem2-101 DBM1-1*), CCY695-10C (*bem2-101 DBM1-2*), CCY886-4C (*bem2-Δ103::LEU2 DBM1-1*), CCY907-16A (*bem2-Δ103::LEU2 DBM1-2*), CCY910-9D × CCY910-12C (*bem2-101/bem2-101 DBM1/DBM1*), CCY447-5C × CCY910-9D (*bem2-101/bem2-101 DBM1-1*/+), and CCY695-10C × CCY910-9D (*bem2-101/bem2-101 DBM1-2*/+).

Nucleotide sequence accession number. The sequence data shown in Fig. 4A are available from the EMBL/GenBank/DDBJ databases under accession number U07421.

RESULTS

The dominant *DBM1-1* and *DBM1-2* mutations can suppress the morphogenesis, actin cytoskeleton, and Ts^- growth defects of *bem2* mutants. To identify gene products that may function with the Bem2 GAP in the regulation of cellular morphogenesis, we have isolated and characterized seven extragenic suppressors of the Ts^- growth phenotype caused by the *bem2-101* mutation (33). Three of these suppressor mutations were found to be dominant (Fig. 1; data not shown). In genetic crosses (CCY109-9C-1* × CCY432-15C and CCY109-9C-1** × CCY432-15C), two of these suppressor mutations were found to be very tightly linked (<4.6 centimorgans) to the *ade2* locus (52 parental ditype:0 nonparental ditype:0 tetratype and 22 parental ditype:0 nonparental ditype:0 tetratype, respectively) present on the right arm of chromosome XV, thus suggesting that these two suppressors represent mutant alleles of the same gene, which we named *DBM1* (dominant suppressor of *bem2*). A description of the third dominant suppressor will be presented elsewhere. To determine whether these two dominant *DBM1* mutations can suppress the *bem2-Δ103*::*LEU2* null mutation, we mated the *bem2-101 DBM1-1 ade2* (CCY447-5C) and *bem2-101 DBM1-2 ade2* (CCY695-10C) strains with a *bem2-Δ103*::*LEU2 DBM1 ADE2* strain (CCY 334-6C). Tetrad analysis of such diploids revealed that *bem2-Δ103*::*LEU2 DBM1-1* (*ade2*) and *bem2-Δ103*::*LEU2 DBM1-2* (*ade2*) cells can grow well at 35°C and, in many cases, also at 37°C (Fig. 1). These results indicate that *DBM1-1* and *DBM1-2*

TABLE 2. Budding patterns and cell morphologies of different haploid yeast strains[a]

Relevant genotype	Temp (°C)	Bud scar pattern (%)			Cell morphology
		A	B	C	
BEM2 DBM1	26	94	2	4	Normal
	37	86	3	11	Normal
BEM2 DBM1-1	26	87	8	5	Elongated
	37	64	14	22	Elongated
BEM2 DBM1-2	26	68	25	7	Elongated
	37	49	25	26	Elongated
bem2-101 DBM1	26	38	9	53	Normal
	37	ND	ND	ND	Round
bem2-101 DBM1-1	26	96	2	2	Elongated
	37	63	18	19	Elongated
bem2-101 DBM1-2	26	95	3	2	Elongated
	37	67	18	15	Elongated
bem2-Δ103::LEU2 DBM1	26	NDQ	NDQ	NDQ	Round
	37	ND	ND	ND	Round
bem2-Δ103::LEU2 DBM1-1	26	87	5	8	Elongated
	37	65	10	25	Elongated
bem2-Δ103::LEU2 DBM1-2	26	87	3	10	Elongated
	37	62	6	32	Elongated
BEM2 dbm1-3::HIS3	26	41	51	8	Normal
	37	35	42	23	Normal
BEM2 dbm1-Δ4::HIS3	26	35	59	6	Normal
	37	30	45	25	Normal

[a] Haploid yeast cells were grown at 26°C in YEPD to a density of ~5×10^6 cells per ml and then shifted to 37°C for 2 h. Cells harvested before and after temperature shift were fixed and then stained with Calcofluor. For each sample, 200 cells with at least two bud scars were scored. In scoring the bud scar pattern, each mother cell body was divided into three equal sectors along its length. Cells with pattern A had bud scars adjacent to each other in only one terminal sector; cells with pattern B had bud scars located in both terminal, but not the middle, sectors; cells with pattern C had bud scars in the middle (and terminal) sector(s). The bud scar pattern of *bem2-Δ103::LEU2 DBM1* cells at 26°C, though clearly randomized in many cases, could not be determined quantitatively (NDQ) because chitin deposition was delocalized in these cells. The bud scar pattern of *bem2 DBM1* cells at 37°C was not determined (ND) because these cells are defective in bud emergence at this temperature. The yeast strains used were CCY482-13D (*BEM2 DBM1*), CCY864-5D (*BEM2 DBM1-1*), CCY919-11B (*BEM2 DBM1-2*), CCY910-12C (*bem2-101 DBM1*), CCY447-5C (*bem2-101 DBM1-1*), CCY695-10C (*bem2-101 DBM1-2*), CCY926-2D (*bem2-Δ103::LEU2 DBM1*), CCY886-4C (*bem2-Δ103::LEU2 DBM1-1*), CCY907-16A (*bem2-Δ103::LEU2 DBM1-2*), CCY814-3A (*BEM2 dbm1-3::HIS3*), and CCY890-12C (*BEM2 dbm1-Δ4::HIS3*).

can suppress the Ts$^-$ growth defect caused by a total loss of Bem2p function.

To determine whether *DBM1-1* and *DBM1-2* also can suppress the morphogenesis defects of *bem2* mutants, we examined budding patterns by Calcofluor staining of cell wall chitin, which is concentrated at bud scars in wild-type cells (28). Our results showed that most haploid *DBM1-1* cells, like wild-type cells, have an axial budding pattern at 26°C, whereas many haploid *DBM1-2* cells bud in a bipolar fashion at this temperature (Table 2 and Fig. 2e). *DBM1-1* and *DBM1-2* cells differ from wild-type cells in being more elongated in shape (Fig. 2a and d). After 2 h at 37°C, the budding pattern is randomized slightly in wild-type cells and more severely in *DBM1-1* or *DBM1-2* cells. While *bem2-101* and *bem2-Δ103::LEU2* cells have a highly randomized budding pattern at 26°C (33) (Table 2 and Fig. 2h), *bem2-101 DBM1-1*, *bem2-101 DBM1-2*, *bem2-Δ103::LEU2 DBM1-1* and *bem2-Δ103::LEU2 DBM1-2* cells bud predominantly in an axial fashion (Fig. 2k). After 2 h at 37°C, delocalized cell surface growth and chitin deposition result in *bem2-101* and *bem2-Δ103::LEU2* cells that are mostly enlarged, round, and unbudded (33) (Fig. 2m). This defect is not observed in *bem2-101 DBM1-1*, *bem2-101 DBM1-2*, *bem2-Δ103::LEU2 DBM1-1*, and *bem2-Δ103::LEU2 DBM1-2* cells, as these cells can bud and remain elongated at 37°C (Fig. 2p). Thus, the *DBM1-1* and *DBM1-2* mutations can suppress the morphogenesis defects caused by a total loss of Bem2p function. Furthermore, this suppression is dominant, as a low-copy-number plasmid carrying the cloned *DBM1-1* allele (see below) can suppress the morphogenesis defects of haploid *bem2-101 DBM1* cells (data not shown). The fact that most haploid *bem2 DBM1-2* double-mutant cells have an axial budding pattern (Table 2) indicates that the mild bipolar bud site selection defect of *DBM1-2* cells also can be suppressed by *bem2* mutations (i.e., reciprocal suppression).

Since *bem2* cells are defective in the organization of a polarized actin cytoskeleton (33) (Fig. 2i and o), we examined the actin cytoskeleton in *DBM1-1* and *DBM1-2* cells by anti-actin immunofluorescence microscopy. At both 26 and 37°C, these cells have a normal-looking actin cytoskeleton that is polarized, with actin cables that run along the mother bud axis and cortical actin patches that are concentrated in the bud (tip) (Fig. 2f and data not shown). Furthermore, *bem2-Δ103::LEU2 DBM1-1* and *bem2-Δ103::LEU2 DBM1-2* cells also have a polarized actin cytoskeleton (Fig. 2l and r and data not shown), thus indicating that the *DBM1-1* and *DBM1-2* mutations can suppress the actin cytoskeletal defects caused by a total loss of Bem2p function.

***DBM1-1* encodes a truncated form of the Dbm1 protein.** To elucidate the molecular basis of the suppression phenomena described above, we carried out a molecular analysis of the *DBM1* gene. Two plasmids (pCC569 and pCC572) containing the *DBM1-1* mutant allele and one plasmid (pCC691) containing wild-type *DBM1* gene were cloned and analyzed (see Materials and Methods) (Fig. 3). Sequencing of these clones revealed that the *DBM1* gene is located near the *ADE2* gene, as predicted from our genetic data. Wild-type *DBM1* potentially encodes a protein of 1,007 residues with a predicted pI of 5.97 and a relative molecular mass of ~113 kDa (Fig. 4A). A DNA segment of 1,747 bp, spanning the region between nucleotides −15 and +1,732 of *DBM1*, is missing from the *DBM1-1* allele. This difference probably resulted from a deletion event mediated by the 6-bp repeats (TGGAGA) that define the deletion endpoints. As a result, the *DBM1-1* allele is predicted to encode a truncated form of the Dbm1 protein, consisting of 378 residues and with a predicted pI of 6.29 and a relative molecular mass of ~43 kDa, assuming that the methionine codon normally present at codon 630 of wild-type *DBM1* is used for translational initiation. In addition, one single-base deletion and nine nucleotide substitutions are found in the *DBM1-1* DNA sequence (Fig. 4A). Five of the nucleotide substitutions are present within the coding region, and they are predicted to result in three amino acid substitutions. These 10 base changes may reflect potential sequence polymorphism of the wild-type *DBM1* locus, since the wild-type *DBM1* gene that was cloned was derived from an existing yeast library constructed with genomic DNA isolated from the strain GRF88 (a derivative of the strain S288C) (62), which is distinct from the parental strain from which the *DBM1-1* mutant allele was derived.

To rule out the possibility that the apparent deletion found in the *DBM1-1* locus also represents potential sequence polymorphism of the wild-type *DBM1* locus, we characterized Dbm1p in wild-type and *DBM1-1* cells. Affinity-purified anti-Dbm1p antibodies used in immunoblotting experiments can recognize three proteins from a yeast extract prepared from the haploid *DBM1* strain from which the *DBM1-1* and *DBM1-2* mutant alleles were derived (Fig. 5, lane b). One of these proteins has an apparent molecular mass of ~110 kDa, which is similar to the predicted molecular mass (~113 kDa) of

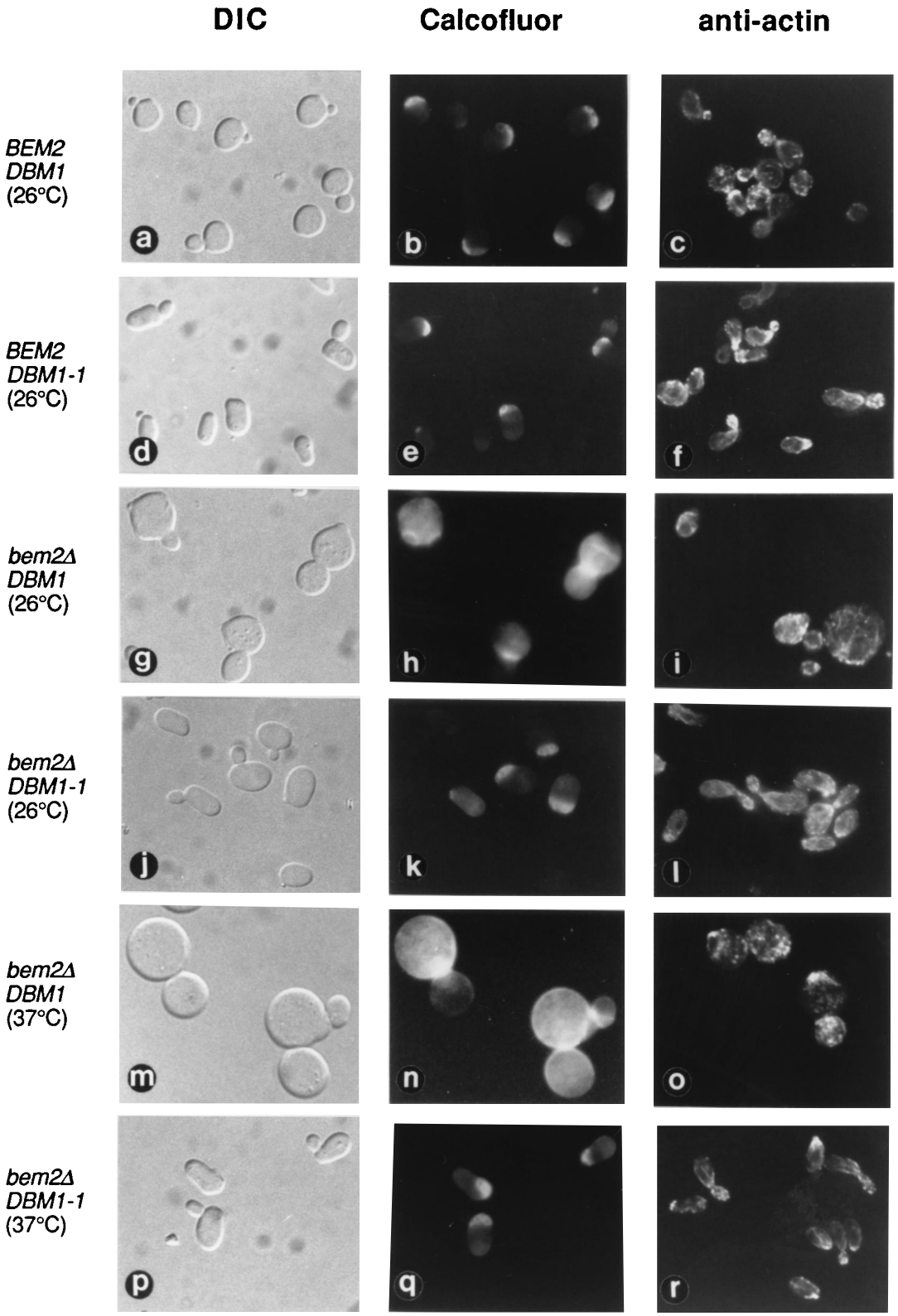

FIG. 2. Cytological examination of *bem2* and *DBM1-1* mutants. Wild-type (CCY482-13D) (a to c), *DBM1-1* (CCY864-5D) (d to f), *bem2-Δ103::LEU2* (CCY926-2D) (g to i and m to o), and *bem2-Δ103::LEU2 DBM1-1* (CCY886-4C) (j to l and p to r) haploid cells grown at 26°C or 37°C for 2 h were fixed and stained with Calcofluor or anti-actin antibodies. The differential interference contrast (DIC) images and the Calcofluor-staining images were obtained from the same cells. All cells are shown at the same magnification.

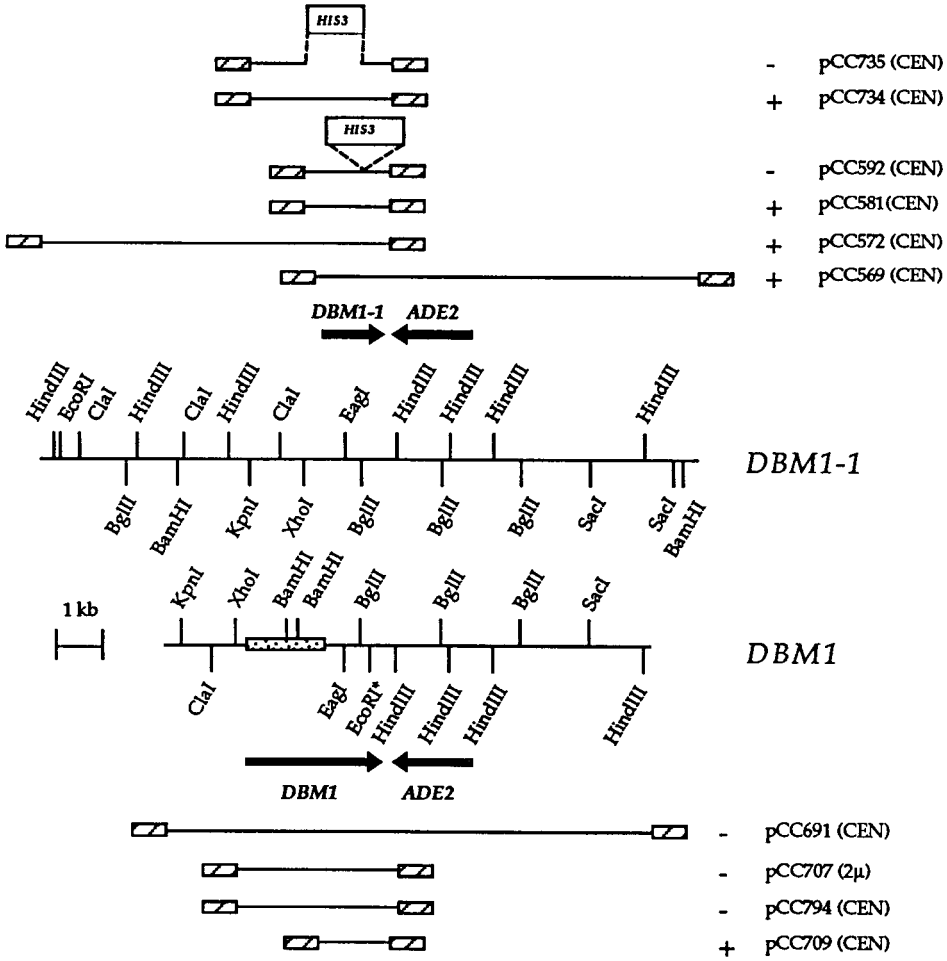

FIG. 3. Functional localization of the *DBM1* and *DBM1-1* alleles. The hatched boxes represent plasmid vector sequences. The stippled box represents DNA sequence not present at the *DBM1-1* locus. The locations and orientations of the predicted *DBM1* (*DBM1-1*) and *ADE2* open reading frames are represented by arrows. The *Eco*RI restriction site found only within the wild-type *DBM1* gene is marked with an asterisk. The ability (+) or inability (−) of the different low-copy-number (CEN) or high-copy-number (2μm) plasmids (containing the DNA fragments shown) to suppress the Ts$^-$ phenotype of a *bem2-101* mutant at 37°C is indicated.

Dbm1p. However, we do not believe that this protein represents intact Dbm1p because it is not detectable in some immunoblotting experiments (data not shown). Instead, it probably represents two protein species, one of which may be a breakdown product of Dbm1p (because its abundance in cells overproducing Dbm1p is increased in some experiments [Fig. 5, lane a]), the other being a protein that cross-reacts in some experiments with the anti-Dbm1p antibodies used (and is thus present even in cells carrying insertion mutations in *DBM1* (Fig. 5, lane e). For two reasons, we believe that the protein with an apparent molecular mass of ~148 kDa represents Dbm1p. First, it is always found in greater abundance in yeast cells that carry the cloned wild-type *DBM1* gene on a high-copy-number plasmid (Fig. 5, lane a). Second, it is totally absent in cells carrying insertion mutations in *DBM1* (Fig. 5, lanes e and f). The apparent molecular mass (~148 kDa) of Dbm1p is significantly higher than the predicted molecular mass (~113 kDa) of this protein. This difference may be due to posttranslational modification, since Dbm1p migrates as a broad band on an SDS-polyacrylamide gel. In *DBM1-1* mutant cells, the ~148-kDa form of Dbm1p is replaced by a form with an apparent molecular mass of ~47 kDa (Fig. 5, lane c), which is similar to the predicted molecular mass (~43 kDa) of the mutant protein encoded by *DBM1-1*. Thus, the deletion found in the *DBM1-1* allele was not caused by a cloning artifact or potential sequence polymorphism of the wild-type *DBM1* gene. Coincidentally, *DBM1-2* mutant cells also contain a form of Dbm1p similar in size to that present in *DBM1-1* cells (Fig. 5, lane d), even though genomic DNA hybridization indicated that *DBM1-2* was caused by a chromosomal rearrangement distinct from the one that yielded *DBM1-1* (data not shown).

Because the level of Dbm1p present in *DBM1-1* and *DBM1-2* mutant cells appears to be elevated (Fig. 5), we examined whether overexpression of wild-type *DBM1* also might result in suppression of *bem2-101*. Our results showed that a high-copy-number plasmid containing *DBM1* (pCC707) cannot suppress the Ts$^-$ phenotype of *bem2-101* cells (Fig. 3). Instead, a low-copy-number plasmid containing a truncated version of wild-type *DBM1* (pCC709) missing sequences upstream of codon 595 can suppress the Ts$^-$ phenotype of such cells. This truncated version of *DBM1* is expected to encode a protein identical to that encoded by *DBM1-1*, assuming that the methionine codon normally present at codon 630 of wild-type *DBM1* is used for translational initiation. This finding suggests that the N-terminal truncation, rather than the three amino acid substitutions, found in Dbm1p encoded by *DBM1-1* may be responsible for the suppression property of this mutant protein.

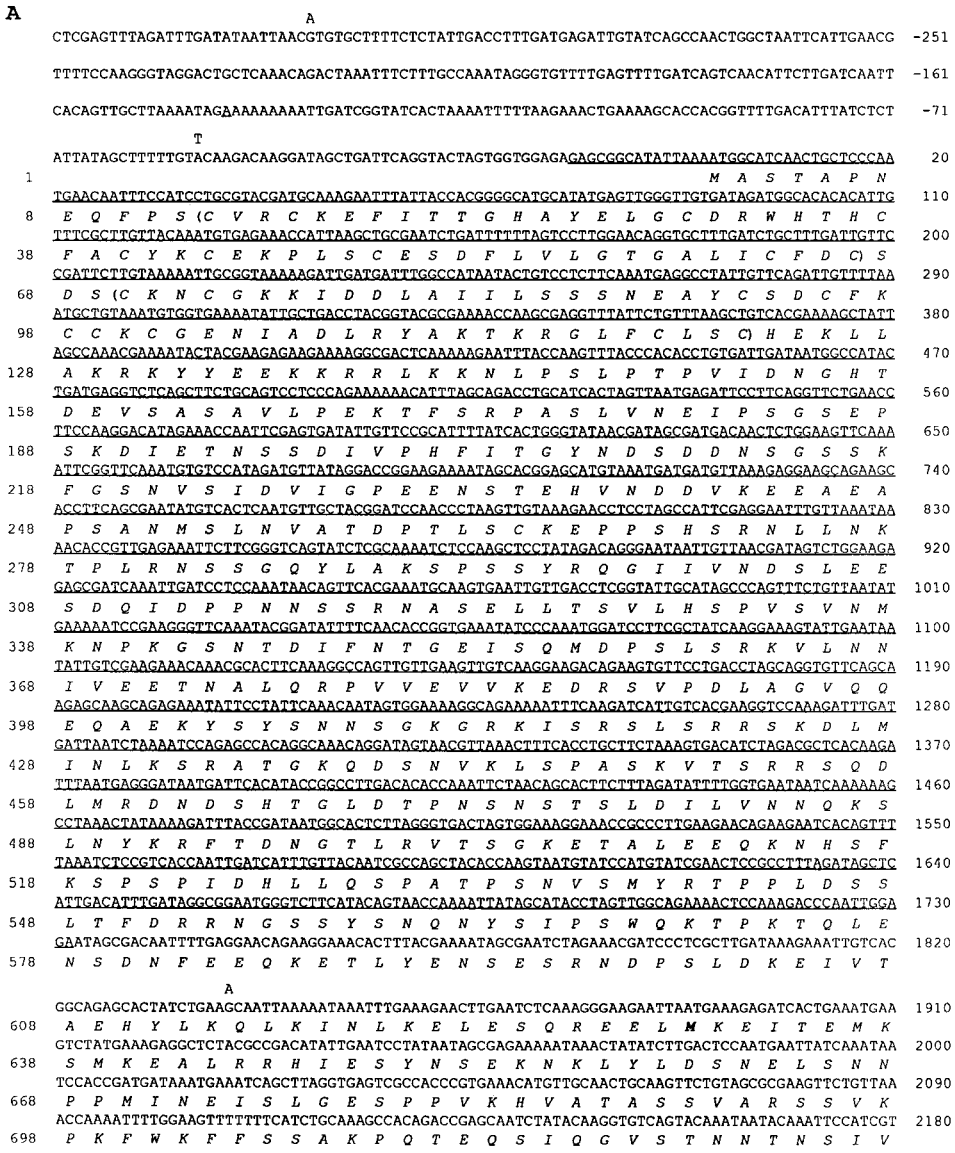

FIG. 4. (A) Nucleotide sequence of the *DBM1* region and predicted amino acid sequence (in italics) of the Dbm1 protein. The nucleotides absent from the *DBM1-1* mutant allele are underlined. The single-base substitutions present in the *DBM1-1* mutant allele are listed above the *DBM1* DNA sequence. The alternative residues predicted to be encoded by the *DBM1-1* mutant allele are listed below the wild-type Dbm1 protein sequence. The methionine codon in boldface represents the putative initiation codon for the forms of the Dbm1 protein encoded by the *DBM1-1* mutant allele and the *THE1* gene fragment. The LIM domains are enclosed in parentheses, and the GAP domain is enclosed in [brackets]. The reverse complement of the 3′ coding sequence of *ADE2* is doubly underlined. (B) Comparison of the LIM domains (lim1 and lim2) found in Dbm1p with the consensus sequence for LIM domains found in other proteins. Identical residues are denoted by vertical lines; similar residues are denoted by colons or periods. Degenerate residues are denoted by X. The most highly conserved residues are numbered 1 to 8. The positions of the cysteine-to-serine substitutions present in mutant Dbm1ps encoded by *dbm1-5*, *-6*, *-7*, and *-8* are also shown.

***DBM1* encodes a putative Rho-Type GAP with two LIM domains.** Comparison of the predicted Dbm1p sequence with known sequences in the GenBank database revealed that codons 569 to 640 of the *DBM1* gene had been sequenced previously as part of the *THE1* gene, which was cloned as a gene fragment that confers growth inhibition in yeast cells when expressed under the control of the *GAL1* promoter (58). Consistent with the potential polymorphic nature of the wild-type *DBM1* DNA sequence proposed above, the single-base substitution present within codon 613 of *DBM1* is also found in the reported *THE1* partial sequence. Interestingly, the *THE1* gene fragment is predicted to encode a truncated form of Dbm1p identical to that encoded by the *DBM1-1* mutant allele (i.e., initiating at codon 630 of wild-type *DBM1*).

Examination of the predicted Dbm1p sequence revealed two interesting features. The region from residues 13 to 122 of wild-type Dbm1p is cysteine rich (Fig. 4). A sequence database search revealed that the cysteine residues present in this region potentially can be organized into two tandemly arranged copies of a sequence motif referred to as the LIM domain (Fig. 4B), which has been identified in a number of proteins, including yeast Lrg1p (49), that are involved in diverse cellular processes (reviewed in reference 67). LIM domains are characterized generally by the presence of eight cysteine and histidine residues that are arranged in a particular order. The second LIM domain (lim2) of Dbm1p differs from most other LIM domains identified so far in that a cysteine residue instead of a histidine residue is present at the third highly conserved posi-

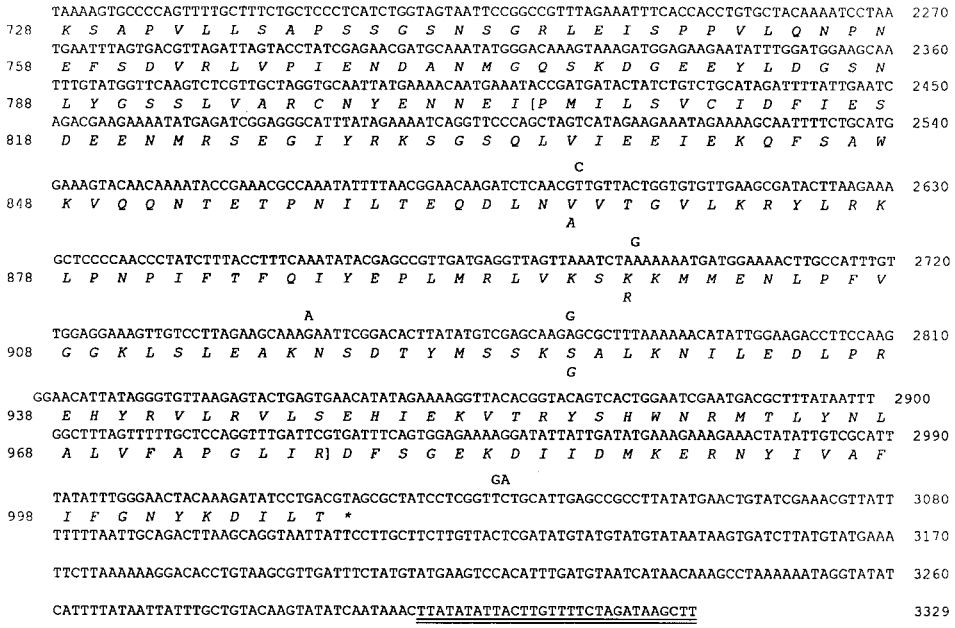

B

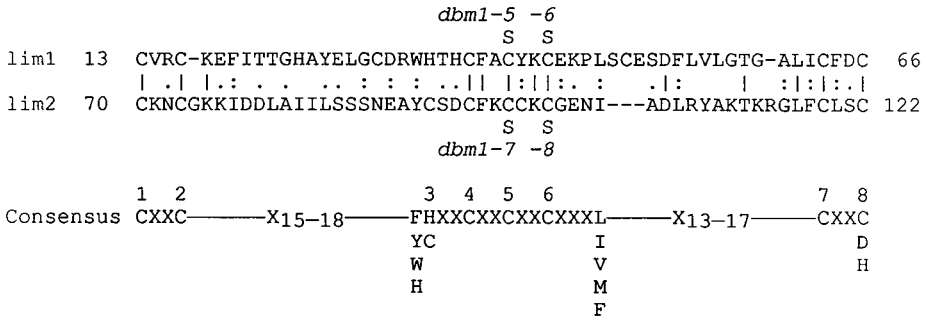

FIG. 4—*Continued.*

tion (Fig. 4B). Interestingly, both LIM domains are absent from the mutant form of Dbm1p encoded by *DBM1-1* (see below). The biochemical properties of LIM domains will be addressed in Discussion.

The COOH-terminal 220 residues of Dbm1p are homologous to sequences found in presumed Rho-type GAPs, including human *n*-chimaerin, Bcr, RhoGAP, and yeast Bem2p, Bem3p, Ybr1728p, Lrg1p, and Uso1p (19, 33, 37, 49, 50, 55, 83, 84). The sequence homology with human *n*-chimaerin is highest (34% identity), and homologies with yeast Bem2p, Bem3p, Ybr1728p, Lrg1p, and Uso1p are lower (29, 31, 24, 21, and 21% identity, respectively). The Dbm1p-related domains from several of these proteins, including yeast Bem2p and human Bcr, have been shown to function in vitro and most probably in vivo as GAPs that are specific for Rho-type GTPases (18, 33, 55, 59, 77). Thus, Dbm1p is a putative Rho-type GAP with two LIM domains. The overall organization of Dbm1p is most similar to that of yeast Lrg1p, which also contains at least two LIM domains as well as a putative GAP domain near its COOH terminus. Furthermore, the three predicted single amino acid substitutions discussed above are all located within the putative GAP domain (Fig. 4A). However, they do not affect residues known to be highly conserved between different Rho-type GAPs. Thus, these substitutions alone may not affect greatly the GAP activity of wild-type or mutant Dbm1p.

***DBM1* itself is required for proper bud site selection.** To determine the importance of Dbm1p for the normal growth of yeast cells, we constructed diploid yeast strains that are heterozygous for the *dbm1-3*::*HIS3* or the *dbm1*-Δ*4*::*HIS3* mutation (see Materials and Methods) (Fig. 3). Tetrad analysis revealed that haploid yeast cells carrying either mutation are viable and have no obvious growth defect on rich medium at temperatures ranging from 13 to 37°C (data not shown). As shown above, immunoblotting experiments revealed that Dbm1p is absent in cells carrying either mutation (Fig. 5). Unlike *DBM1-1* and *DBM1-2* cells, cells lacking Dbm1p are normal in shape (Fig. 6 and Table 2). Thus, Dbm1p is not essential for cell viability or cell shape control in cells grown on YEPD rich medium. However, bud site selection is abnormal in haploid *dbm1*-Δ*4*::*HIS3* and *dbm1-3*::*HIS3* cells. Calcofluor-staining of bud scars showed that as many as 50 to 60% of such cells assume a bipolar budding pattern characteristic of wild-type diploid cells and a smaller fraction assume an even more randomized budding pattern (Fig. 6g and Table 2). Diploid cells homozygous for the *dbm1*-Δ*4*::*HIS3* or *dbm1-3*::*HIS3* mutation, like wild-type diploid cells, bud in a bipolar fashion (data not shown). Thus, Dbm1p is essential for proper bud site selection in haploid but not diploid cells. Furthermore, a much smaller fraction of *dbm1*-Δ*4*::*HIS3* haploid cells than of wild-type cells appear to have multiple bud scars. For example, in

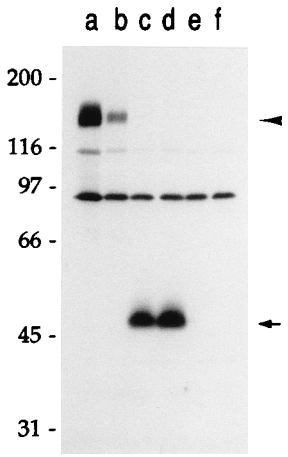

FIG. 5. Identification of Dbm1p in wild-type cells and *DBM1* mutants. Roughly equal amounts of yeast whole cell lysates prepared from different strains were separated on an SDS–10% polyacrylamide gel and used for immunoblotting with affinity-purified anti-Dbm1p antibodies. Yeast strains used: lane a, CCY482-13D (*BEM2 DBM1*) carrying *DBM1* on a high-copy-number plasmid (pCC707); lane b, CCY109-9C-1 (*bem2-101 DBM1*); lane c, CCY109-9C-1* (*bem2-101 DBM1-1*); lane d, CCY109-9C-1** (*bem2-101 DBM1-2*); lane e, CCY814-3A (*BEM2 dbm1-3*::*HIS3*); lane f, CCY890-12C (*BEM2 dbm1-Δ4*::*HIS3*). The arrowhead and arrow highlight wild-type Dbm1p encoded by *DBM1* and mutant Dbm1p encoded by *DBM1-1* or *DBM1-2*, respectively.

one experiment, ~40% of wild-type cells, but only ~8% of *dbm1-Δ4*::*HIS3* cells, have two or more bud scars. This observation suggests that *dbm1-Δ4*::*HIS3* cells may have a tendency not to bud more than once, which would be expected to result in a greatly increased doubling time. However, this appears not to be true because wild-type and *dbm1-Δ4*::*HIS3* cells seem to have comparable growth rates and cell cycle distributions (data not shown). Furthermore, microscopic observation of the budding pattern of single cells on agar plates (14) showed that *dbm1-Δ4*::*HIS3* cells are indeed defective in bud site selection and that they do not have a tendency to bud only once. Thus, the reason why *dbm1-Δ4*::*HIS3* cells appear to have fewer bud scars remains to be elucidated.

Since *AXL1*, mutations of which also result in a bipolar budding pattern, is expressed only in haploid cells (24), we examined the potential cell type control of *DBM1* expression by immunoblotting. Our results showed that the expression of *DBM1* is not haploid cell specific because similar levels of Dbm1p are found in haploid and diploid cells (data not shown). To examine whether Dbm1p may be required for the control of other aspects of polarized cell growth, we also examined the ability of haploid *dbm1-Δ4*::*HIS3* cells to form mating projections (shmoos) in response to mating pheromone. Our results showed that these cells can produce mating projections that appear normal, and they have no measurable mating defect (data not shown). This latter observation distinguishes *dbm1* mutants from *lrg1Δ459-753*::*HIS3* mutants, which exhibit a 1,000-fold reduction in mating efficiency as a

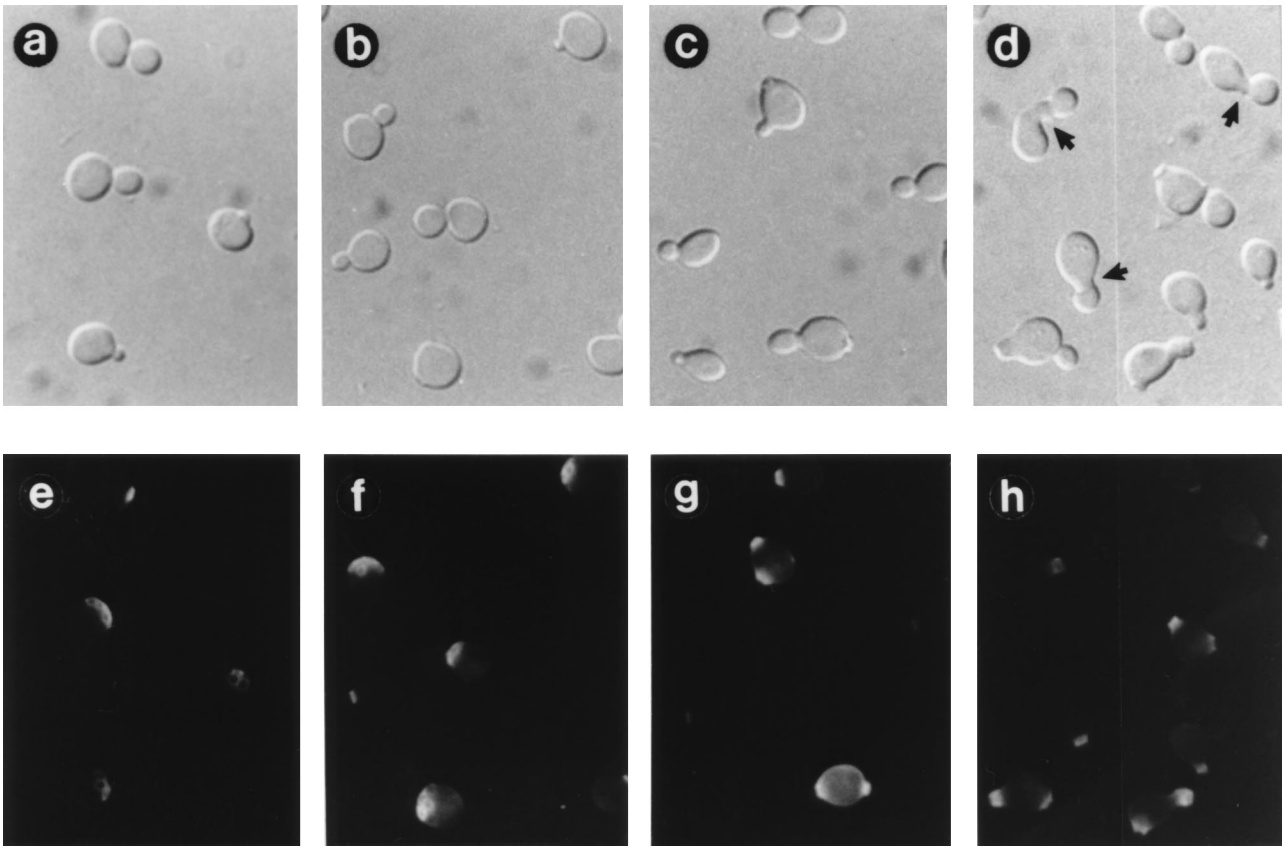

FIG. 6. *dbm1 bem3* double mutants are abnormal in shape. Wild-type (CCY898-25B) (a and e), *bem3*::*LEU2* (CCY898-25A) (b and f), *dbm1-Δ4*::*HIS3* (CCY898-25C) (c and g), and *bem3*::*LEU2 dbm1-Δ4*::*HIS3* (CCY898-25D) (d and h) haploid cells grown at 26°C were stained with Calcofluor. The differential interference contrast images (a to d) and Calcofluor-staining images (e to h) were obtained from the same cells. The arrows in panel d highlight the broad and extended bud necks seen in many *bem3*::*LEU2 dbm1-Δ4*::*HIS3* cells.

result of the absence of Lrg1p, which is structurally related to Dbm1p (49). It also suggests that the predominantly bipolar budding pattern of haploid *dbm1* cells is not due to the expression of both **a** and α information at *HM* loci, as observed in haploid *sir* mutant cells (60).

Dbm1p and Bem2p together are essential for cell viability. Since *DBM1* and *BEM2* both encode GAP domain-containing proteins that are required for proper bud site selection, we examined the consequence of simultaneous inactivation of both genes. Tetrad analysis of a diploid strain (CBY1830-30-13) homozygous for *his3* and *leu2* and heterozygous for *dbm1-3*::*HIS3* and *bem2-Δ103*::*LEU2* revealed that *dbm1-3*::*HIS3 bem2-Δ103*::*LEU2* double mutants are inviable at 26°C on YEPD rich medium. Among 28 tetrads analyzed, none of the viable spores were His^+ Leu^+. Four tetrads produced four viable spores, all of which were His^+ Leu^- or His^- Leu^+ (i.e., parental ditype). Three tetrads produced two viable spores that were His^- Leu^- (i.e., nonparental ditype). Twenty-one tetrads produced three viable spores; 18 of these 21 tetrads produced viable spores that were His^+ Leu^-, His^- Leu^+, or His^- Leu^- (i.e., tetratype). Among the 27 inviable spores, 24 had the inferred genotype of *dbm1-3*::*HIS3 bem2-Δ103*::*LEU2*. Similar results were obtained when tetrads from a diploid strain (CCY825-2) heterozygous for the *dbm1-Δ4*::*HIS3* and *bem2-Δ103*::*LEU2* mutations were analyzed (data not shown). Thus, when assayed for the ability to affect the growth phenotype caused by the *bem2-Δ103*::*LEU2* mutation, the *dbm1-3*::*HIS3* and *dbm1-Δ4*::*HIS3* loss-of-function alleles have properties exactly opposite those of the *DBM1-1* and *DBM1-2* dominant alleles (see Discussion). The observed synthetic lethal phenotype caused by a combination of *bem2-Δ103*::*LEU2* and *dbm1-3*::*HIS3* or *dbm1-Δ4*::*HIS3* mutations suggests that Dbm1p and Bem2p perform similar or overlapping functions that are required for cell viability.

It is known that the Ts^- growth defect of *bem2-Δ103*::*LEU2* mutants can be suppressed partially by the presence of an osmotic stabilizing agent in the growth medium (33). We were interested in knowing whether the inviability phenotype of *dbm1-3*::*HIS3 bem2-Δ103*::*LEU2* and *dbm1-Δ4*::*HIS3 bem2-Δ103*::*LEU2* mutants also could be rescued by this perturbation. The tetrad analyses described above were repeated on YEPD rich medium that contained sorbitol (at 1 M) as an osmotic stabilizer, and results similar to those shown above were obtained. Examination of the inviable His^+ Leu^+ cells by light microscopy revealed that these cells either failed to germinate or lysed after germination even in the presence of sorbitol. Thus, the synthetic lethal phenotype caused by a combination of *bem2-Δ103*::*LEU2* and *dbm1-3*::*HIS3* or *dbm1-Δ4*::*HIS3* mutations cannot be suppressed by the presence of an osmotic stabilizer, suggesting that this perturbation cannot suppress the *dbm1-3*::*HIS3* and *dbm1-Δ4*::*HIS3* mutations.

The bud site selection defect of *dbm1-Δ4*::*HIS3* mutants can be rescued by an increase in the dosage of *BEM3* but not *BEM2*. *BEM3*, like *BEM2* and presumably *DBM1*, encodes a Rho-type GAP (83). Several lines of evidence indicate that *BEM2* and *BEM3* are functionally related. First, the GAP domains of both Bem2p and Bem3p stimulate the GTPase activity of Rho1p in vitro (55, 83). Second, high-copy-number plasmids containing *BEM3* can suppress the Ts^- phenotype of *bem2* mutants (6). Third, the *bem3*::*LEU2* null mutation exacerbates the Ts^- phenotype of *bem2-Δ110*::*TRP1* cells (our unpublished results). Thus, we also determined the functional relationship of *BEM3* and *DBM1* in the following ways. First, we examined the consequence of simultaneous inactivation of both genes. Tetrad analysis of a diploid strain (CBY1830-45-1) homozygous for *his3* and *leu2* and heterozygous for *dbm1-Δ4*::*HIS3* and *bem3*::*LEU2* revealed that *dbm1-Δ4*::*HIS3 bem3*::*LEU2* double mutants are viable on YEPD rich medium and have no obvious growth defects at temperatures ranging from 13 to 37°C, thus indicating that Dbm1p and Bem3p together do not perform a function essential for cell viability. However, many *dbm1-Δ4*::*HIS3 bem3*::*LEU2* double-mutant cells are abnormal in shape, with the bud neck of ~40% of budded cells being unusually broad, curved, and/or elongated (Fig. 6d). Bud scar staining is often quite diffuse, and in some instances, a double ring of chitin staining can be seen at some bud necks. The latter unusual staining pattern may not be apparent in Fig. 6h.

TABLE 3. Budding patterns of haploid cells carrying different combinations of *dbm1-Δ4*::*HIS3* and *bem3*::*LEU2* mutations[a]

Strain	Relevant genotype	Bud scar pattern (%)		
		A	B	C
CCY898-25B	*DBM1 BEM3*	93	0	7
CCY898-25A	*DBM1 bem3*::*LEU2*	92	1	7
CCY898-25C	*dbm1-Δ4*::*HIS3 BEM3*	31	56	13
CCY898-25D	*dbm1-Δ4*::*HIS3 bem3*::*LEU2*	6	75	19

[a] Haploid cells from one complete tetrad derived from a diploid strain (CBY1830-45-1) heterozygous for *dbm1-Δ4*::*HIS3* and *bem3*::*LEU2* were grown at 26°C to a density of ~5×10^6 cells per ml in YEPD. These cells were fixed and then stained with Calcofluor. For each sample, 700 cells with at least two bud scars were scored, using the same criteria as those described for Table 2.

Furthermore, examination of the bud scar pattern of haploid *dbm1-Δ4*::*HIS3 bem3*::*LEU2* double-mutant cells revealed that they have a more abnormal budding pattern than *dbm1-Δ4*::*HIS3* single-mutant cells, since a much smaller fraction of double-mutant cells bud in the normal axial fashion (Table 3). The very low level of *dbm1-Δ4*::*HIS3 bem3*::*LEU2* double-mutant cells that exhibit an axial budding pattern distinguishes such cells from other bud site selection mutants that exhibit a bipolar budding pattern (e.g., *axl1* [24]), and it suggests that *dbm1-Δ4*::*HIS3 bem3*::*LEU2* double-mutant cells may have a strong bias against using the same pole for successive budding cycles. A similar bias has been previously observed when wild-type haploid cells that are in stationary phase are diluted into fresh medium, and it has been suggested that cell cycle delays may promote this bias (42). However, there is no evidence that *dbm1-Δ4*::*HIS3 bem3*::*LEU2* double-mutant (CCY898-25D) cells exhibit cell cycle delays because their doubling time at 26°C in YEPD rich medium (~127 min) is similar to that of wild-type (CCY898-25B) and *dbm1-Δ4*::*HIS3* single mutant (CCY898-25C) cells (~123 and ~125 min, respectively).

We also examined the consequence of increasing the dosage of *BEM3* in *dbm1-Δ4*::*HIS3* cells. Our results showed that a high-copy-number *BEM3* plasmid can suppress the nonaxial budding defect of *dbm1-Δ4*::*HIS3* cells (Table 4). These observations together suggest that Bem3p and Dbm1p may perform similar or overlapping functions in vivo. Interestingly, similar analysis showed that a high-copy-number *BEM2* plasmid not only fails to suppress the nonaxial budding defect of *dbm1-Δ4*::*HIS3* cells but actually results in a more randomized budding pattern in these (but not wild-type) cells (Table 4 and data not shown), thus indicating that Dbm1p function cannot be replaced by that of Bem2p.

The bud site selection defect of *dbm1-Δ4*::*HIS3* mutants is exacerbated by an increase in the dosage of *CDC42*. Since Bem2p functions in vitro as a GAP for the Rho1 but not the Cdc42 GTPase whereas Bem3p functions in vitro as a GAP for both GTPases, albeit with different efficiencies (55, 83, 84), the genetic interactions observed between *BEM2*, *BEM3*, and

TABLE 4. Budding patterns of *dbm1-Δ4*::*HIS3* haploid cells overexpressing different GAPs[a]

Plasmid	Relevant features	Bud scar pattern (%)		
		A	B	C
pSM218	2μm, *LEU2*	59	37	4
pCC554	2μm, *LEU2*, *BEM2*	51	18	31
pPB547	2μm, *LEU2*, *BEM3*	84	14	2

[a] Haploid *dbm1-Δ4*::*HIS3 ura3 leu2* (CCY890-12C) cells carrying different plasmids were grown at 26°C to a density of ~5 × 10^6 cells per ml in SD supplemented with adenine, uracil, histidine, and tryptophan (i.e., lacking leucine). These cells were fixed and then stained with Calcofluor. For each sample, 200 cells with at least two bud scars were scored, using the same criteria as those described for Table 2.

DBM1 as well as the predicted sequence of Dbm1p suggest that Dbm1p also may function as a GAP for Cdc42p, Rho1p, and/or other Rho-type GTPases. To address this possibility, we examined the effect on bud site selection when each of the five known yeast Rho-type GTPases (Rho1p, Rho2p, Rho3p, Rho4p, and Cdc42p) was moderately overproduced. Our results showed that the presence of a high-copy-number *CDC42* plasmid causes, as previously reported (30), a partial defect in bud site selection in wild-type cells (Table 5) and that this plasmid further exacerbates the bud site selection defect of *dbm1-Δ4*::*HIS3* cells. One interpretation for these results is that Dbm1p functions in vivo as a GAP for Cdc42p and that overproduction of Cdc42p in cells lacking Dbm1p results in an even greater excess of Cdc42p that is in the GTP-bound, and presumably active, state. In contrast, high-copy-number plasmids carrying *RHO3* or *RHO4* do not noticeably affect bud site selection in wild-type or *dbm1-Δ4*::*HIS3* cells, thus suggesting that Dbm1p may not play a role in the regulation of Rho3p and Rho4p. The results obtained from high-copy-number plasmids carrying *RHO1* or *RHO2* are less clear. While these plasmids do not affect bud site selection in wild-type cells, they appear to exacerbate slightly the bud site selection defects of *dbm1-Δ4*::*HIS3* cells. However, because the perturbation caused by overproduction of Rho1p and Rho2p is relatively minor, we think that Dbm1p plays at most a minor role in the regulation of these two GTPases.

TABLE 6. Budding patterns of *dbm1-Δ4*::*HIS3* haploid cells carrying different plasmids[a]

Plasmid	Relevant gene	Amino acid substitution(s)	Bud scar pattern (%)		
			A	B	C
pRS316			59	35	6
pCC794	*DBM1*		88	11	1
pCC795	*dbm1-5*	C40S	66	29	5
pCC801	*dbm1-6*	C43S	68	31	1
pCC800	*dbm1-7*	C98S	62	32	6
pCC799	*dbm1-8*	C101S	67	31	2
pCC796	*dbm1-5,7*	C40S, C98S	64	30	6
pCC797	*dbm1-5,7,8*	C40S, C98S, C101S	66	29	5

[a] Haploid *dbm1-Δ4*::*HIS3 ura3* (CCY862-5B) cells carrying different low-copy-number *URA3*-CEN plasmids were grown at 26°C in SD supplemented with adenine and Casamino Acids (i.e., lacking uracil) to a density of ~5 × 10^6 cells per ml, fixed, and then stained with Calcofluor. For each sample, 300 cells with at least two bud scars were scored, using the same criteria as those described for Table 2. Plasmids pCC794 to pCC801 are identical except for the mutations noted.

Both LIM domains are important for normal Dbm1p function. The two LIM domains (lim1 and lim2) of wild-type Dbm1p are located within the N-terminal 122 residues, which are absent from mutant Dbm1p encoded by *DBM1-1* (Fig. 4). Thus, we were interested in knowing whether these LIM domains may be important for normal Dbm1p function. For this purpose, we used site-directed mutagenesis to create a series of *dbm1* mutant alleles. The *dbm1-5* and *dbm1-6* alleles encode mutant Dbm1p with the cysteine residues present at the conserved positions 5 and 6, respectively, of lim1 substituted by the structurally similar serine residue; the *dbm1-7* and *dbm1-8* alleles encode Dbm1p with similar substitutions at conserved positions 5 and 6 of lim2, respectively (Fig. 4B). The properties of these mutant alleles were assayed in the following ways.

First, we examined whether low-copy-number plasmids that carried the different *dbm1* LIM domain mutant alleles could restore normal budding pattern in *dbm1-Δ4*::*HIS3* cells. As shown in Table 6, the nonaxial budding defect of haploid *dbm1-Δ4*::*HIS3* cells is complemented by a low-copy-number plasmid that carries wild-type *DBM1*. In contrast, none of the

TABLE 5. Budding patterns of wild-type and *dbm1-Δ4*::*HIS3* haploid cells overexpressing different Rho-type GTPases[a]

Strain	Plasmid	Relevant gene(s)	Bud scar pattern (%)		
			A	B	C
DBM1	pSM217	*URA3*	93.4 ± 0.6	1.3 ± 1.5	5.3 ± 1.2
	pCC707	*URA3*, *DBM1*	94.7 ± 2.9	0.3 ± 0.6	5.0 ± 2.6
	YEpU-CDC42	*URA3*, *CDC42*	86.0 ± 3.6	6.7 ± 1.2	7.3 ± 2.5
	YEpU-RHO1	*URA3*, *RHO1*	95.0 ± 1.0	1.7 ± 2.1	3.3 ± 1.2
	YEpU-RHO2	*URA3*, *RHO2*	94.3 ± 0.6	1.0 ± 1.0	4.7 ± 1.5
	pOPR3	*URA3*, *RHO3*	94.7 ± 0.6	2.0 ± 1.0	3.3 ± 0.6
	pOPR4	*TRP1*, *RHO4*	92.3 ± 1.2	2.0 ± 0.0	5.7 ± 1.2
dbm1-Δ4::*HIS3*	pSM217	*URA3*	52.0 ± 2.6	41.3 ± 3.1	6.7 ± 0.6
	pCC707	*URA3*, *DBM1*	94.3 ± 0.6	0.7 ± 0.6	5.0 ± 1.0
	YEpU-CDC42	*URA3*, *CDC42*	37.0 ± 5.2	53.7 ± 4.2	9.3 ± 1.5
	YEpU-RHO1	*URA3*, *RHO1*	47.7 ± 4.5	41.0 ± 4.6	11.3 ± 1.2
	YEpU-RHO2	*URA3*, *RHO2*	45.3 ± 3.1	46.7 ± 4.0	8.0 ± 2.6
	pOPR3	*URA3*, *RHO3*	54.3 ± 2.1	40.4 ± 2.1	5.3 ± 2.1
	pOPR4	*TRP1*, *RHO4*	51.3 ± 6.1	39.7 ± 6.7	9.0 ± 1.7

[a] Haploid *dbm1-Δ4*::*HIS3 ura3 trp1* (CCY890-12C) or *DBM1 ura3 trp1* (DBY1828) cells carrying different high-copy-number plasmids were grown at 26°C to a density of ~5 × 10^6 cells per ml in SD supplemented with Casamino Acids, adenine, and uracil or tryptophan (i.e., lacking tryptophan or uracil, respectively). These cells were fixed and then stained with Calcofluor. For each sample, 200 cells with at least two bud scars were scored in each experiment, using the same criteria as those described for Table 2. The means and standard deviations from three independent experiments are shown.

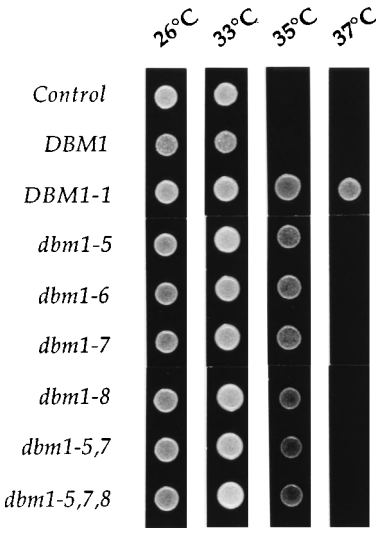

FIG. 7. Suppression of the Ts⁻ growth phenotype of a *bem2-101* mutant by different *dbm1* LIM domain mutations. Suspensions of *bem2-101* (CCY416-12D) cells carrying different low-copy-number *URA3*-CEN plasmids were spotted on YEPD plates and allowed to grow at the indicated temperatures for 2 days. Apart from pCC581, which carried the *DBM1-1* mutant allele, the plasmids used were identical to those listed in Table 6.

plasmids that carry *dbm1* LIM domain mutant alleles can significantly alter the nonaxial budding pattern of *dbm1-Δ4::HIS3* cells, even though wild-type levels of mutant Dbm1p are present in these cells (data not shown). Second, we examined whether the different *dbm1* LIM domain mutant alleles could suppress the bud site selection and Ts⁻ growth defects of *bem2* cells. As shown in Fig. 7, *bem2-101* cells containing low-copy-number plasmids pCC795 to pCC801 can grow at 35°C, thus indicating that each *dbm1* LIM domain mutation tested can suppress the Ts⁻ phenotype of *bem2-101* mutants, even when wild-type *DBM1* is present. However, suppression is incomplete because *bem2-101* cells fail to grow at 37°C, even when they contain high-copy-number plasmids that carry the different *dbm1* LIM domain mutant alleles (data not shown). Similar analysis showed that each of these *dbm1* mutant alleles also can suppress the Ts⁻ growth defect of *bem2-Δ103::LEU2* single mutants at 33°C and the inviability of *bem2-Δ103::LEU2 dbm1-Δ4::HIS3* double mutants at 26°C (data not shown). Thus, substitution of a single conserved cysteine residue in either one of the two LIM domains within Dbm1p abolishes the ability of this protein to perform its normal function in bud site selection and yet confers on mutant Dbm1p the ability to provide a function (needed for bud emergence) that is lacking in *bem2* cells. Interestingly, none of the *dbm1* LIM domain mutations tested can suppress the bud site selection defect of *bem2-101* cells (data not shown), thus suggesting that the bud site selection and bud emergence functions of Bem2p may be separable.

DISCUSSION

The Dbm1, Bem2, and Bem3 GAPs together are needed for proper polarized cell growth. Previous studies of *S. cerevisiae* mutants defective in cellular morphogenesis have identified Bem2p as an important component that controls polarized cell growth in yeast cells. In this report, we show that the control of polarized cell growth also involves Dbm1p, which contains at its COOH-terminal end a GAP domain similar to that found in Bem2p. Loss of Dbm1p function results in a bipolar budding pattern in haploid cells. Two lines of evidence suggest that Dbm1p and Bem2p perform similar or overlapping functions in vivo. First, cells lacking both Dbm1p and Bem2p have a synthetic lethal phenotype not seen in loss-of-function *dbm1* and *bem2* single mutants. Second, the dominant *DBM1-1* mutation, which encodes a truncated form of Dbm1p lacking its N-terminal end but still containing the GAP domain, can suppress the bud site selection and Ts⁻ growth defects of mutant cells that totally lack Bem2p. However, Dbm1p and Bem2p are not functionally equivalent because overproduction of wild-type Dbm1p does not result in the suppression of *bem2* mutant phenotypes and overproduction of Bem2p actually exacerbates the nonaxial budding defect of *dbm1* mutants (Table 4). In addition to Dbm1p and Bem2p, the control of polarized cell growth also involves Bem3p, which also contains at its COOH-terminal end a GAP domain similar to that found in Bem2p and Dbm1p (83). The Ts⁻ phenotype of *bem2* mutants is suppressed by an increase in the dosage of *BEM3* (6), and the Ts⁻ phenotype of *bem2-Δ110::TRP1* mutant cells is exacerbated by the *bem3::LEU2* null mutation (our unpublished results). Similarly, the nonaxial budding defect of *dbm1* mutants is suppressed strongly by an increase in the dosage of *BEM3* (Table 4) and is exacerbated by a loss of Bem3p function (Table 3 and Fig. 6).

Which GTPase is regulated by Dbm1p in vivo? Since the GAP domain of Bem3p functions in vitro as a GAP for Cdc42p, and less effectively also for Rho1p (83, 84), whereas the GAP domain of Bem2p functions in vitro as a GAP for Rho1p but not Cdc42p (55, 83, 84), the genetic interactions between *BEM2*, *BEM3*, and *DBM1* may be interpreted in at least two ways. First, the GTPase activity of Rho1p (and possibly Rho2p) may be stimulated in vivo by the combination of Bem2p, Bem3p, and Dbm1p, with the latter two proteins playing smaller roles since *bem3* mutant cells have no discernible morphogenesis or growth defects (83) (Table 3) and *dbm1* mutant cells, unlike *bem2* mutant cells, are not Ts⁻ for growth or defective in bud emergence. Consistent with this possibility are the observations that *dbm1* null mutations cause a synthetic lethal phenotype in *bem2-Δ103::LEU2* cells whereas *bem3* null mutations only exacerbate the Ts⁻ phenotype of *bem2-Δ103::LEU2* cells (our unpublished results). Since *bem2* mutant phenotype is partially suppressed by an increase in the dosage of *RHO1* (or *RHO2*) (33) and is exacerbated by certain *rho1* mutations (reference 77 and our unpublished results), we might expect the *dbm1* mutant phenotype to be similarly affected by such perturbations if both Bem2p and Dbm1p function in vivo as GAPs for Rho1p (and Rho2p). We found this not to be true because an increase in the dosage of *RHO1* (or *RHO2*) perhaps very mildly exacerbates (rather than suppresses) the *dbm1* mutant phenotype (Table 5), and the Ts⁻ phenotype of $rho1^{G121C}$ mutant cells (50a) is not affected noticeably by an increase in the dosage of *DBM1* or by the *dbm1-Δ4::HIS3* mutation (our unpublished results). These observations argue that if both Dbm1p and Bem2p stimulate the GTPase activity of Rho1p (or Rho2) in vivo, they must do so in distinctly different ways.

An alternative interpretation for our genetic data is that Dbm1p, like Bem3p, functions as a GAP for Cdc42p and that the morphogenesis defects caused by loss of Bem2p function (and the presumed associated perturbation of Rho1p function) may be compensated for by perturbations of Cdc42p function caused by overproduction of Bem3p (which can also function in vitro as a GAP for Rho1p) or by mutational alteration (e.g., N-terminal truncation) of Dbm1p (see below). Consistent with this interpretation are the observations that an increase in the gene dosage of *CDC42* as well as the *bem3::LEU2* mutation

exacerbate the bud site selection defect of *dbm1* cells (Table 5). If this interpretation is correct, Dbm1p probably plays a more important role than Bem3p in the regulation of Cdc42p because *dbm1* mutants, unlike *bem3* mutants, are defective in bud site selection, a phenotype also observed when Cdc42p is overproduced (Table 5). Furthermore, Dbm1p and Bem3p may not be the only GAPs that regulate Cdc42p in vivo because *dbm1 bem3* double mutants are viable, whereas *cdc42* mutant alleles that are predicted to encode Cdc42p with reduced GTPase activity cause a dominant lethal phenotype (86). Clearly, the two interpretations discussed so far do not have to be mutually exclusive. It is possible that Dbm1p can function as a GAP for both Cdc42p and Rho1p (and possibly Rho2p) in vivo, and the degree to which any one of these GTPases is regulated by Dbm1p may be dictated at least partly by the subcellular localization of Dbm1p and the different GTPases (see below). For example, Dbm1p may normally function mainly as a GAP for Cdc42p. Thus, the absence of Dbm1p (as in *dbm1* null-mutant cells) results in a bud site selection defect similar to that caused by the overproduction of Cdc42p. However, when Dbm1p is present but mislocalized (e.g., as a result of N-terminal truncation), it may function more as a GAP for Rho1p (and possibly Rho2p), thus reducing the requirement for Bem2p.

Recently, *DBM1* has also been identified independently as a gene (named *RGA1*) that functions as a negative regulator in the pheromone response pathway (74). In two-hybrid interaction trap assays, the GAP domain of Dbm1p/Rga1p interacts strongly with Cdc42p and much less strongly with Rho1p. These latter results are consistent with our proposed function for Dbm1p.

The LIM domains of Dbm1p may regulate its biological function. While much remains to be learned about the in vivo functions of Dbm1p, our studies indicate that both of the LIM domains that are present in tandem near the N-terminal end of this protein are required for its normal function. LIM domains are characterized by eight highly conserved and appropriately spaced cysteine and histidine residues (Fig. 4B). Biochemical and biophysical studies have shown that the LIM domains of a number of proteins can bind zinc (4, 29, 38, 45, 65, 68), and they may mediate intermolecular protein-protein interactions (20) or intramolecular interactions (66, 80). Thus, LIM domains may serve as regulatory domains of some proteins.

We have created mutant forms of Dbm1p with serine substituting for one or both of the cysteine residues present at conserved positions 5 and 6 in either one or both of the LIM domains (Fig. 4B). These mutant LIM domains are not expected to bind any zinc atom or to fold correctly (35, 46). Yeast cells with any one of these mutant forms of Dbm1p as their only source of Dbm1p bud predominantly in a bipolar fashion, just like cells that totally lack Dbm1p (Table 6), thus indicating that both of the LIM domains of Dbm1p are required for its normal function. Furthermore, the Ts^- growth phenotype of *bem2-101* mutants is partially suppressed by the production of any one of these mutant forms of Dbm1p even when wild-type Dbm1p is also present (Fig. 7). This observation suggests that the LIM domains of Dbm1p may play a regulatory role in this protein, perhaps serving to localize Dbm1p through intermolecular interaction(s) with another protein(s). In this model, the LIM domain mutant forms of Dbm1p may be mislocalized, thus precluding them from performing the function normally carried out by wild-type Dbm1p and simultaneously conferring on it the ability to perform the function normally carried out by Bem2p. Alternatively, the LIM domains of Dbm1p may serve to control its specificity toward different GTPases, perhaps through intramolecular interactions with another functional domain within Dbm1p. In this model, the LIM domain mutant forms of Dbm1p may have altered substrate specificity (e.g., functioning as more effective GAPs for Rho1p instead of Cdc42p) even though they are properly localized. Both of these models are consistent with the observation that overproduction of wild-type Dbm1p does not result in the suppression of the *bem2* mutant phenotype. In this context, it is interesting that the mutant form of Dbm1p encoded by *DBM1-1*, which lacks both LIM domains as well as the N-terminal 62% of wild-type Dbm1p, can provide both Dbm1p and Bem2p functions since *DBM1-1 BEM2* and *DBM1-1 bem2-Δ103::LEU2* cells, unlike *dbm1-Δ4::HIS3* and *bem2-Δ103::LEU2* cells, have normal budding patterns (Table 2), thus suggesting that another regulatory domain may exist within the N-terminal 62% of Dbm1p.

ACKNOWLEDGMENTS

We thank Jon Mulholland for the supply of anti-actin antibodies, Alan Bender for the supply of *BEM3* plasmids, Yoshi Ohya for the supply of the $rho1^{G121C}$ mutant, John Pringle and George Sprague for communication of results before publication, and Alison Adams and Brian Haarer for comments on the manuscript.

This work was supported by National Institutes of Health grant GM45185 and Advanced Research Program grant 003658-510 from The Texas Higher Education Coordinating Board.

REFERENCES

1. **Adames, N., K. Blundell, M. N. Ashby, and C. Boone.** 1995. Role of yeast insulin-degrading enzyme homologs in propheromone processing and bud site selection. Science **270:**464–467.
2. **Adams, A. E. M., D. I. Johnson, R. M. Longnecker, B. F. Sloat, and J. R. Pringle.** 1990. *CDC42* and *CDC43*, two additional genes involved in budding and the establishment of cell polarity in the yeast *Saccharomyces cerevisiae*. J. Cell Biol. **111:**131–142.
3. **Adams, A. E. M., and J. R. Pringle.** 1984. Relationship of actin and tubulin distribution in wild-type and morphogenetic mutant *Saccharomyces cerevisiae*. J. Cell Biol. **98:**934–945.
4. **Archer, V. E. V., J. Breton, I. Sanchez-Garcia, H. Osada, A. Forster, A. J. Thomson, and T. H. Rabbitts.** 1994. Cysteine-rich LIM domains of LIM-homeodomain and LIM-only proteins contain zinc but not iron. Proc. Natl. Acad. Sci. USA **91:**316–320.
5. **Bender, A.** 1993. Genetic evidence for the roles of the bud-site-selection genes *BUD5* and *BUD2* in control of the Rsr1p (Bud1p) GTPase in yeast. Proc. Natl. Acad. Sci. USA **90:**9926–9929.
6. **Bender, A., and J. Pringle.** 1991. Use of a screen for synthetic lethal and multicopy suppressee mutants to identify two new genes involved in morphogenesis in *Saccharomyces cerevisiae*. Mol. Cell. Biol. **11:**1295–1305.
7. **Bender, A., and J. R. Pringle.** 1989. Multicopy suppression of the *cdc24* budding defect in yeast by *CDC42* and three newly identified genes including the *ras*-related gene *RSR1*. Proc. Natl. Acad. Sci. USA **86:**9976–9980.
8. **Benton, B. K., A. H. Tinkelenberg, D. Jean, S. D. Plump, and F. R. Cross.** 1993. Genetic analysis of Cln/Cdc28 regulation of cell morphogenesis in budding yeast. EMBO J. **12:**5267–5275.
9. **Bretscher, A., B. Drees, E. Harsay, D. Schott, and T. Wang.** 1994. What are the basic functions of microfilaments? Insights from studies in budding yeast. J. Cell Biol. **126:**821–825.
10. **Brewster, J. L., and M. C. Gustin.** 1994. Positioning of cell growth and division after osmotic stress requires a MAP kinase pathway. Yeast **10:**425–439.
11. **Chan, C. S. M., and D. Botstein.** 1993. Isolation and characterization of chromosome-gain and increase-in-ploidy mutants in yeast. Genetics **135:** 677–691.
12. **Chant, J.** 1994. Cell polarity in yeast. Trends Genet. **10:**328–333.
13. **Chant, J., K. Corrado, J. R. Pringle, and I. Herskowitz.** 1991. Yeast *BUD5*, encoding a putative GDP-GTP exchange factor, is necessary for bud site selection and interacts with bud formation gene *BEM1*. Cell **65:**1213–1224.
14. **Chant, J., and I. Herskowitz.** 1991. Genetic control of bud site selection in yeast by a set of gene products that constitute a morphogenetic pathway. Cell **65:**1203–1212.
15. **Chant, J., M. Mischke, E. Mitchell, I. Herskowitz, and J. R. Pringle.** 1995. Role of Bud3p in producing the axial budding pattern of yeast. J. Cell Biol. **129:**767–778.
16. **Chant, J., and J. R. Pringle.** 1995. Patterns of bud-site selection in the yeast *Saccharomyces cerevisiae*. J. Cell Biol. **129:**751–765.
17. **Chenevert, J., K. Corrado, A. Bender, J. Pringle, and I. Herskowitz.** 1992. A yeast gene (*BEM1*) necessary for cell polarization whose product contains two SH3 domains. Nature (London) **356:**77–79.

17a. **Corrado, K.** Personal communication.
18. **Diekmann, D., S. Brill, M. D. Garrett, N. Totty, J. Hsuan, C. Monfries, C. Hall, L. Lim, and A. Hall.** 1991. *Bcr* encodes a GTPase-activating protein for $p21^{rac}$. Nature (London) **351:**400–402.
19. **Doignon, F., N. Biteau, M. Crouzet, and M. Aigle.** 1993. The complete sequence of a 19,482 bp segment located on the right arm of chromosome II from *Saccharomyces cerevisiae*. Yeast **9:**189–199.
20. **Feuerstein, R., X. Wang, D. Song, N. E. Cooke, and S. A. Liebhaber.** 1994. The LIM/double zinc-finger motif functions as a protein dimerization domain. Proc. Natl. Acad. Sci. USA **91:**10655–10659.
21. **Flescher, E. G., K. Madden, and M. Snyder.** 1993. Components required for cytokinesis are important for bud site selection in yeast. J. Cell Biol. **122:** 373–386.
22. **Ford, S. K., and J. R. Pringle.** 1991. Cellular morphogenesis in the *Saccharomyces cerevisiae* cell cycle: localization of the *CDC11* gene product and the timing of events at the budding site. Dev. Genet. **12:**281–292.
23. **Friefelder, D.** 1960. Bud position in *Saccharomyces cerevisiae*. J. Bacteriol. **80:**567–568.
24. **Fujita, A., C. Oka, Y. Arikawa, T. Katagai, A. Tonouchi, S. Kuhara, and Y. Misumi.** 1994. A yeast gene necessary for bud-site selection encodes a protein similar to insulin-degrading enzymes. Nature (London) **372:**567–570.
25. **Gimeno, C. J., P. O. Ljungdahl, C. A. Styles, and G. R. Fink.** 1992. Unipolar cell divisions in the yeast *S. cerevisiae* lead to filamentous growth: regulation by starvation and *RAS*. Cell **68:**1077–1090.
26. **Haarer, B. K., and J. R. Pringle.** 1987. Immunofluorescence localization of the *Saccharomyces cerevisiae CDC12* gene product to the vicinity of the 10-nm filaments in the mother-bud neck. Mol. Cell. Biol. **7:**3678–3687.
27. **Hall, A.** 1994. Small GTP-binding proteins and the regulation of the actin cytoskeleton. Annu. Rev. Cell Biol. **10:**31–54.
28. **Hayashibe, M., and S. Katohda.** 1973. Initiation of budding and chitin-ring. J. Gen. Appl. Microbiol. **19:**23–39.
29. **Hempe, J. M., and R. J. Cousins.** 1991. Cysteine-rich intestinal protein binds zinc during transmucosal zinc transport. Proc. Natl. Acad. Sci. USA **88:**9671–9674.
30. **Johnson, D. I., and J. R. Pringle.** 1990. Molecular characterization of *CDC42*, a *Saccharomyces cerevisiae* gene involved in the development of cell polarity. J. Cell Biol. **111:**143–152.
31. **Jones, J. S., and L. Prakash.** 1990. Yeast *Saccharomyces cerevisiae* selectable markers in pUC18 polylinkers. Yeast **6:**363–366.
32. **Kim, H. B., B. K. Haarer, and J. R. Pringle.** 1991. Cellular morphogenesis in the *Saccharomyces cerevisiae* cell cycle: localization of the *CDC3* gene product and the timing of events at the budding site. J. Cell Biol. **112:**535–544.
33. **Kim, Y.-J., L. Francisco, G.-C. Chen, E. Marcotte, and C. S. M. Chan.** 1994. Control of cellular morphogenesis by the Ipl2/Bem2 GTPase-activating protein: possible role of protein phosphorylation. J. Cell Biol. **127:**1381–1394.
34. **Koerner, T. J., J. E. Hill, A. M. Myers, and A. Tzagoloff.** 1991. High-expression vectors with multiple cloning sites for construction of trpE fusion genes: pATH vectors. Methods Enzymol. **194:**477–490.
35. **Kosa, J. L., J. W. Michelsen, H. A. Louis, J. I. Olsen, D. R. Davis, M. C. Beckerle, and D. R. Winge.** 1994. Common metal ion coordination in LIM domain proteins. Biochemistry **33:**468–477.
36. **Kunkel, T. A., J. D. Roberts, and R. A. Zakour.** 1987. Rapid and efficient site-specific mutagenesis without phenotypic selection. Methods Enzymol. **154:**367–382.
37. **Lamarche, N., and A. Hall.** 1994. GAPs for rho-related GTPases. Trends Genet. **10:**436–440.
38. **Li, P. M., J. Reichert, G. Freyd, H. R. Horvitz, and C. T. Walsh.** 1991. The LIM region of a presumptive *Caenorhabditis elegans* transcription factor is an iron-sulfur- and zinc-containing metallodomain. Proc. Natl. Acad. Sci. USA **88:**9210–9213.
39. **Li, R., Y. Zheng, and D. G. Drubin.** 1995. Regulation of cortical actin cytoskeleton assembly during polarized cell growth in budding yeast. J. Cell Biol. **128:**599–615.
40. **Madaule, P., R. Axel, and A. M. Myers.** 1987. Characterization of two members of the *rho* gene family from the yeast *Saccharomyces cerevisiae*. Proc. Natl. Acad. Sci. USA **84:**779–783.
41. **Madden, K., C. Costigan, and M. Snyder.** 1992. Cell polarity and morphogenesis in *Saccharomyces cerevisiae*. Trends Cell Biol. **2:**22–29.
42. **Madden, K., and M. Snyder.** 1992. Specification of sites for polarized growth in *Saccharomyces cerevisiae* and the influence of external factors on site selection. Mol. Biol. Cell **3:**1025–1035.
43. **Marmur, J.** 1961. A procedure for the isolation of deoxyribonucleic acid from micro-organisms. J. Mol. Biol. **3:**208–218.
44. **Matsui, Y., and A. Toh-e.** 1992. Yeast *RHO3* and *RHO4 ras* superfamily genes are necessary for bud growth, and their defect is suppressed by a high dose of bud formation genes *CDC42* and *BEM1*. Mol. Cell. Biol. **12:**5690–5699.
45. **Michelsen, J. W., K. L. Schmeichel, M. C. Beckerle, and D. R. Winge.** 1993. The LIM motif defines a specific zinc-binding protein domain. Proc. Natl. Acad. Sci. USA **90:**4404–4408.
46. **Michelsen, J. W., A. K. Sewell, H. A. Louis, J. I. Olsen, D. R. Davis, D. R. Winge, and M. C. Beckerle.** 1994. Mutational analysis of the metal sites in an LIM domain. J. Biol. Chem. **269:**11108–11113.
47. **Molero, G., M. Yuste-Rojas, A. Montesi, A. Vázquez, C. Nombela, and M. Sanchez.** 1993. A cdc-like autolytic *Saccharomyces cerevisiae* mutant altered in budding site selection is complemented by *SPO12*, a sporulation gene. J. Bacteriol. **175:**6562–6570.
48. **Mulholland, J., D. Preuss, A. Moon, A. Wong, D. Drubin, and D. Botstein.** 1994. Ultrastructure of the yeast actin cytoskeleton and its association with the plasma membrane. J. Cell Biol. **125:**381–391.
49. **Müller, L., G. Xu, R. Wells, C. P. Hollenberg, and W. Piepersberg.** 1994. LRG1 is expressed during sporulation in Saccharomyces cerevisiae and contains motifs similar to LIM and rho/racGAP domains. Nucleic Acids Res. **22:**3151–3154.
50. **Nakajima, H., A. Hirata, Y. Ogawa, T. Yonehara, K. Yoda, and M. Yamasaki.** 1991. A cytoskeleton-related gene, *USO1*, is required for intracellular protein transport in *Saccharomyces cerevisiae*. J. Cell Biol. **113:**245–260.
50a. **Ohya, Y.** Personal communication.
51. **Ohya, Y., S. Miyamoto, Y. Ohsumi, and Y. Anraku.** 1986. Calcium-sensitive *cls4* mutant of *Saccharomyces cerevisiae* with a defect in bud formation. J. Bacteriol. **165:**28–33.
52. **Ohya, Y., Y. Ohsumi, and Y. Anraku.** 1984. Genetic study of the role of calcium ions in the cell division cycle of *Saccharomyces cerevisiae*: a calcium-dependent mutant and its trifluoperazine-dependent pseudorevertants. Mol. Gen. Genet. **193:**389–394.
53. **Ohya, Y., H. Qadota, Y. Anraku, J. R. Pringle, and D. Botstein.** 1993. Suppression of yeast geranylgeranyl transferase I defect by alternative prenylation of two target GTPases, Rho1p and Cdc42p. Mol. Biol. Cell **4:**1017–1025.
54. **Park, H.-O., J. Chant, and I. Herskowitz.** 1993. *BUD2* encodes a GTPase-activating protein for Bud1/Rsr1 necessary for proper bud-site selection in yeast. Nature (London) **365:**269–274.
55. **Peterson, J., Y. Zheng, L. Bender, A. Myers, R. Cerione, and A. Bender.** 1994. Interactions between the bud emergence proteins Bem1p and Bem2p and Rho-type GTPases in yeast. J. Cell Biol. **127:**1395–1406.
56. **Powers, S., E. Gonzales, T. Christensen, J. Cubert, and D. Broek.** 1991. Functional cloning of *BUD5*, a *CDC25*-related gene from *S. cerevisiae* that can suppress a dominant-negative *RAS2* mutant. Cell. **65:**1225–1231.
57. **Pringle, J. R., R. A. Preston, A. Adams, T. Stearns, D. Drubin, B. K. Haarer, and E. Jones.** 1989. Fluorescence microscopy methods for yeast. Methods Cell Biol. **31:**357–435.
58. **Ramer, S. W., S. J. Elledge, and R. W. Davis.** 1992. Dominant genetics using a yeast genomic library under the control of a strong inducible promoter. Proc. Natl. Acad. Sci. USA **89:**11589–11593.
59. **Ridley, A. J., A. J. Self, F. Kasmi, H. F. Paterson, A. Hall, C. J. Marshall, and C. Ellis.** 1993. rho family GTPase activating proteins p190, bcr and rhoGAP show distinct specificities *in vitro* and *in vivo*. EMBO J. **12:**5151–5160.
60. **Rine, J., and I. Herskowitz.** 1987. Four genes responsible for a position effect on expression from HML and HMR in *Saccharomyces cerevisiae*. Genetics **116:**9–22.
61. **Roberts, R. L., and G. R. Fink.** 1994. Elements of a single MAP kinase cascade in *Saccharomyces cerevisiae* mediate two developmental programs in the same cell type: mating and invasive growth. Genes Dev. **8:**2974–2985.
62. **Rose, M. D., P. Novick, J. H. Thomas, D. Botstein, and G. R. Fink.** 1987. A *Saccharomyces cerevisiae* genomic plasmid bank based on a centromere-containing shuttle vector. Gene **60:**237–243.
63. **Rose, M. D., F. Winston, and P. Hieter.** 1990. Methods in yeast genetics. Cold Spring Harbor Laboratory Press, Cold Spring Harbor, N.Y.
64. **Rothstein, R. J.** 1983. One-step gene disruption in yeast. Methods Enzymol. **101:**202–211.
65. **Sadler, I., A. W. Crawford, J. W. Michelsen, and M. C. Beckerle.** 1992. Zyxin and cCRP: two interactive LIM domain proteins associated with the cytoskeleton. J. Cell Biol. **119:**1573–1587.
66. **Sánchez-García, I., H. Osada, A. Forster, and T. H. Rabbitts.** 1993. The cysteine-rich LIM domains inhibit DNA binding by the associated homeodomain in Isl-1. EMBO J. **12:**4243–4250.
67. **Sánchez-García, I., and T. H. Rabbits.** 1994. The LIM domain: a new structural motif found in zinc-finger-like proteins. Trends Genet. **10:**315–320.
68. **Schmeichel, K. L., and M. C. Beckerle.** 1994. The LIM domain is a modular protein-binding interface. Cell **79:**211–219.
69. **Sikorski, R. S., and P. Hieter.** 1989. A system of shuttle vectors and yeast host strains designed for efficient manipulation of DNA in *Saccharomyces cerevisiae*. Genetics **122:**19–27.
70. **Sloat, B. F., A. Adams, and J. R. Pringle.** 1981. Roles of the *CDC24* gene product in cellular morphogenesis during the *Saccharomyces cerevisiae* cell cycle. J. Cell Biol. **89:**395–405.
71. **Sloat, B. F., and J. R. Pringle.** 1978. A mutant of yeast defective in cellular morphogenesis. Science **200:**1171–1173.
72. **Snyder, M.** 1989. The *SPA2* protein of yeast localizes to sites of cell growth. J. Cell Biol. **108:**1419–1429.
73. **Snyder, M., S. Gehrung, and B. D. Page.** 1991. Studies concerning the temporal and genetic control of cell polarity in *Saccharomyces cerevisiae*. J. Cell Biol. **114:**515–532.

74. **Stevenson, B. J., B. Ferguson, C. De Virgilio, E. Bi, J. R. Pringle, G. Ammerer, and G. F. Sprague Jr.** 1995. Mutation of *RGA1*, which encodes a putative GTPase-activating protein for the polarity—establishment protein Cdc42p, activates the pheromone response pathway in the yeast *Saccharomyces cerevisiae*. Genes Dev. **9:**2949–2963.
75. **Takai, Y., T. Sasaki, K. Tanaka, and H. Nakanishi.** 1995. Rho as a regulator of the cytoskeleton. Trends Biochem. Sci. **20:**227–231.
76. **Trueblood, C. E., Y. Ohya, and J. Rine.** 1993. Genetic evidence for in vivo cross-specificity of the CaaX-box protein prenyltransferases farnesyltransferase and geranylgeranyltransferase I in *Saccharomyces cerevisiae*. Mol. Cell. Biol. **13:**4260–4275.
77. **Wang, T., and A. Bretscher.** 1995. The *rho*-GAP encoded by *BEM2* regulates cytoskeletal structure in budding yeast. Mol. Biol. Cell **6:**1011–1024.
78. **Welch, M. D., D. A. Holtzman, and D. G. Drubin.** 1994. The yeast actin cytoskeleton. Curr. Opin. Cell Biol. **6:**110–119.
79. **Winey, M., M. A. Hoyt, C. Chan, L. Goetsch, D. Botstein, and B. Byers.** 1993. *NDC1*: a nuclear periphery component required for yeast spindle pole body duplication. J. Cell Biol. **122:**743–751.
80. **Xue, D., Y. Tu, and M. Chalfie.** 1993. Cooperative interactions between the *Caenorhabditis elegans* homeoproteins UNC-86 and MEC-3. Science. **261:** 1324–1328.
81. **Yamochi, W., K. Tanaka, H. Nonaka, A. Maeda, T. Musha, and Y. Takai.** 1994. Growth site localization of Rho1 small GTP-binding protein and its involvement in bud formation in *Saccharomyces cerevisiae*. J. Cell Biol. **125:** 1077–1093.
82. **Zheng, Y., A. Bender, and R. A. Cerione.** 1995. Interactions among proteins involved in bud-site selection and bud-site assembly in *Saccharomyces cerevisiae*. J. Biol. Chem. **270:**626–630.
83. **Zheng, Y., R. Cerione, and A. Bender.** 1994. Control of the yeast bud-site assembly GTPase Cdc42: catalysis of guanine-nucleotide exchange by Cdc24 and stimulation of GTPase activity by Bem3. J. Biol. Chem. **269:**2369–2372.
84. **Zheng, Y., M. J. Hart, K. Shinjo, T. Evans, A. Bender, and R. A. Cerione.** 1993. Biochemical comparisons of the *Saccharomyces cerevisiae* Bem2 and Bem3 proteins. J. Biol. Chem. **268:**24629–24634.
85. **Ziman, M., and D. I. Johnson.** 1994. Genetic evidence for a functional interaction between *Saccharomyces cerevisiae CDC24* and *CDC42*. Yeast. **10:**463–474.
86. **Ziman, M., J. M. O'Brien, L. A. Ouellette, W. R. Church, and D. I. Johnson.** 1991. Mutational analysis of *CDC42Sc*, a *Saccharomyces cerevisiae* gene that encodes a putative GTP-binding protein involved in the control of cell polarity. Mol. Cell. Biol. **11:**3537–3544.
87. **Ziman, M., D. Preuss, J. Mulholland, J. M. O'Brien, D. Botstein, and D. I. Johnson.** 1993. Subcellular localization of Cdc42p, a *Saccharomyces cerevisiae* GTP-binding protein involved in the control of cell polarity. Mol. Biol. Cell **4:**1307–1316.